

# INVESTIGATION OF THE EFFECT OF FIXED ABSORBERS ON THE REACTIVITY OF PWR SPENT NUCLEAR FUEL FOR BURNUP CREDIT

JOHN C. WAGNER\* and CHARLOTTA E. SANDERS  
*Oak Ridge National Laboratory, P.O. Box 2008  
Oak Ridge, Tennessee 37831-6370*

Received August 14, 2001

Accepted for Publication February 22, 2002

*The effect of fixed absorbers on the reactivity of pressurized water reactor (PWR) spent nuclear fuel (SNF) in support of burnup-credit criticality safety analyses is examined. A fuel assembly burned in conjunction with fixed absorbers may have a higher reactivity for a given burnup than an assembly that has not used fixed absorbers. As a result, guidance on burnup credit, issued by the U.S. Nuclear Regulatory Commission's Spent Fuel Project Office, recommends restricting the use of burnup credit to assemblies that have not used burnable absorbers. This recommendation eliminates a large portion of the currently discharged SNF from loading in burnup credit casks and thus severely limits the practical usefulness of*

*burnup credit. Therefore, data are needed to support the extension of burnup credit to additional SNF. This research investigates the effect of various fixed absorbers, including integral burnable absorbers, burnable poison rods, control rods, and axial power shaping rods, on the reactivity of PWR SNF. Trends in reactivity with relevant parameters (e.g., initial fuel enrichment, burnup and absorber type, exposure, and design) are established, and anticipated reactivity effects are quantified. Where appropriate, recommendations are offered for addressing the reactivity effects of the fixed absorbers in burnup-credit safety analyses.*

## I. INTRODUCTION

The concept of taking credit for the reduction in reactivity of burned or spent nuclear fuel (SNF) due to fuel burnup is commonly referred to as burnup credit. The reduction in reactivity that occurs with fuel burnup is due to the change in concentration (net reduction) of fissile nuclides and the production of actinide and fission product neutron absorbers. The change in the concentration of these nuclides with fuel burnup, and consequently the reduction in reactivity, is dependent on the depletion environment (e.g., the neutron spectrum). As a result, the utilization of credit for fuel burnup necessitates consideration of variations in fuel designs and operating conditions, including the use of fixed absorbers.

The presence of fixed absorbers in a light water reactor fuel assembly lattice during depletion hardens the neutron spectrum, resulting in increased production of fissile plutonium isotopes and reduced  $^{235}\text{U}$  depletion. Consequently, a fuel assembly burned in conjunction with fixed absorbers may have a higher reactivity for a given burnup than an assembly that has not used fixed absorbers. Therefore, where fixed absorbers have been employed, computational predictions of SNF reactivity (e.g., for burnup credit) must consider the impact of their presence.

Although currently approved SNF storage and transportation casks are licensed under the fresh-fuel assumption, in which all fuel assemblies are conservatively assumed to be unirradiated in the criticality safety evaluation, credit for fuel burnup is currently being pursued for SNF storage, transportation, and disposal applications as a means to maximize SNF cask capacities and

\*E-mail: wagnerjc@ornl.gov

improve design flexibility. In support of burnup credit for these applications, this research investigates the effect of various fixed absorbers, including integral burnable absorbers (IBAs), burnable poison rods (BPRs), control rods (CRs), and axial power shaping rods (APSRs), on the reactivity of pressurized water reactor (PWR) SNF. The analyses and data presented herein may help facilitate the storage, transportation, and disposal of additional older SNF assemblies and those to be discharged in the future.

### I.A. Background

Continuing advancements in fuel assembly design have enabled enhanced fuel utilization, thereby increasing the performance of reactor cores (i.e., extending core lifetimes). One characteristic of these advanced fuel assembly designs is the expanded use of fixed burnable absorber (neutron poison) materials, either as an integral part of the fuel assembly or as a separate (removable) assembly used in conjunction with the fuel assembly. For the purpose of this discussion, burnable absorbers are classified into two distinct categories: BPRs and IBAs. BPRs are rods containing neutron-absorbing material that may be inserted into the guide tubes of a PWR assembly. BPRs have most frequently been used with fresh fuel assemblies during their first burnup cycle. In contrast to BPRs, IBAs refer to burnable poisons that are a nonremovable or integral part of the fuel assembly once it is manufactured. An example of an IBA is the Westinghouse integral fuel burnable absorber (IFBA) rod, which has a coating of zirconium diboride ( $ZrB_2$ ) on a select number of the fuel pellets. In general, recent trends in PWR fuel management have shifted away from the use of BPRs and toward increased use of IBAs. However, BPRs, which have been used extensively in the past, are still being used in a few PWRs in the United States and may find renewed usage with mixed oxide fuel.

Control rods and APSRs are fixed absorbers, similar to BPRs in that they also contain neutron-absorbing material and may be inserted into the guide tubes of a PWR assembly. However, while BPRs are used to improve fuel utilization, CRs are primarily used in U.S. PWRs for reactor control during startup and shutdown operations and are not typically inserted (to a significant extent) into the guide tubes during normal operation. Depending on plant-specific fuel management strategies, CRs may be either completely withdrawn or partially inserted (e.g., for reactor control or load-following) during normal operations. Axial power shaping rods are generally classified with CRs but may differ in their design and usage; APSRs are generally shorter in length and may be inserted for extended periods of burnup. Due to their respective compositions and usage, CRs and APSRs are not considered burnable because their compositions are not significantly depleted.

In the past, criticality safety evaluations for spent-fuel storage and transportation canisters<sup>1,2</sup> assumed the spent fuel to be fresh (unburned) fuel with uniform isotopics corresponding to the maximum allowable enrichment. This fresh-fuel assumption provides a well-defined bounding approach to the criticality safety analysis that eliminates concerns related to the fuel operating history, thereby considerably simplifying the analysis. However, in July of 1999, the U.S. Nuclear Regulatory Commission's (NRC) Spent Fuel Project Office issued an interim staff guidance<sup>3</sup> on burnup credit (ISG-8) that allows partial credit for burnup in PWR fuel. Subsequently, the guidance in ISG-8 was integrated into the standard review plan for transportation packages.<sup>4</sup> The recommendations in Refs. 3 and 4 limit the amount of burnup credit to that available from actinide compositions in irradiated PWR  $UO_2$  fuel up to an assembly-average burnup of 40 Gwd/tonne U, with a number of associated restrictions. These recommendations include a restriction on the use of burnup credit to assemblies that have not used burnable absorbers and a note of particular concern with the "need to consider the more reactive actinide compositions of fuels burned with fixed absorbers or with control rods fully or partly inserted." As burnable absorbers and CRs are routinely used in PWRs, this recommended restriction eliminates a large portion of the current and future SNF inventory from cask loading with burnup credit and thus severely limits the practical usefulness of burnup credit.

In the absence of comprehensive studies on the effects of fixed absorbers on the reactivity of SNF and readily available information on the design specifications and usage of fixed absorbers in U.S. PWRs, NRC staff has indicated<sup>5</sup> a need for greater understanding in these areas. In support of this need, a research project was initiated to (a) accumulate information on fixed absorber designs and usage, and (b) perform computational studies to investigate the effect of fixed absorbers on the reactivity of PWR SNF. This paper presents a summary of numerous studies<sup>6-8</sup> that have been performed to establish and quantify the effect of fixed absorbers on the reactivity of SNF for various absorber types and designs, fuel enrichments, and exposure conditions. For brevity, this paper presents the most significant aspects of the analyses to demonstrate trends and support conclusions. The interested reader is referred to Refs. 6, 7, and 8 for additional comparisons, detailed absorber and fuel design specifications, and recommendations for addressing the use of fixed absorbers in burnup-credit safety evaluations.

### I.B. Outline

The remainder of this paper is organized as follows. Section II describes the methodology used for this computational investigation. Sections III, IV, and V present individual analyses for IBAs, BPRs, and CRs,

respectively. Trends in reactivity with relevant parameters, such as initial fuel enrichment, burnup, and absorber exposure and design, are established and anticipated reactivity effects are quantified. As APSRs are considered by many to be a type of CR, discussions and analyses for CRs and APSRs are presented together in Sec. V. Summary and conclusions are provided in Sec. VI.

## II. METHODOLOGY

The vast majority of the calculations presented in the following sections were performed using the HELIOS-1.6 code package.<sup>9</sup> HELIOS is a two-dimensional (2-D) transport theory code based on the method of collision probabilities with current coupling. HELIOS was employed for this analysis because of its capability to explicitly model the relatively complicated, heterogeneous assembly lattices associated with IBAs, BPRs, and CRs. The various structures within each of the models were coupled using angular current discretization (interface currents), and all calculations utilized the 45-group neutron cross-section library (based on ENDF/B-VI) that is distributed with the HELIOS-1.6 code package.

The depletion calculations were performed using reasonably conservative cycle-averaged operational parameters for fuel temperature (1000 K), moderator temperature (600 K), soluble boron concentration (650 ppm), and specific power (60 MW/tonne U). The sensitivity of neutron multiplication to variations in these parameters is discussed in Ref. 10. Using the isotopic compositions from the depletion calculations, branch or restart calculations were performed with HELIOS to determine the infinite neutron multiplication factor  $k_{inf}$  as a function of burnup for out-of-reactor conditions (i.e., unborated moderator at 20°C).

Unless specifically stated otherwise, all HELIOS criticality calculations correspond to an infinite radial array

of assemblies at zero cooling time and include all of the actinide and fission product nuclides available in the HELIOS cross-section library; the reason for using zero cooling time and all nuclides is calculational simplicity. Where exceptions are made to study the impact of various relevant conditions and configurations, such as cooling time and cask geometry, they are clearly stated. For studies that require three-dimensional (3-D) analysis, criticality calculations were performed with the KENO V.a Monte Carlo code<sup>11</sup> from the SCALE package<sup>12</sup> using spent-fuel isotopics calculated by HELIOS. The KENO V.a calculations used the 238-group cross-section library, based primarily on ENDF/B-V data.

Unlike the HELIOS criticality calculations, which include all of the actinide and fission product nuclides available in the HELIOS cross-section library, the KENO criticality calculations were performed with subsets of the available nuclides. The use of a subset of possible actinides in burnup credit calculations is referred to as actinide-only burnup credit. The nuclides used here for actinide-only calculations are consistent with those specified in a U.S. Department of Energy (DOE) topical report on burnup credit,<sup>13</sup> with the exception that <sup>236</sup>U and <sup>237</sup>Np are also included. While not consistently defined elsewhere, the use of a subset of possible actinides and fission products is referred to herein as actinide + fission product burnup credit. The fission product nuclides used here for actinide + fission product calculations are consistent with those identified in Table 2 of Ref. 14 as being the most important for criticality calculations. Table I lists the nuclides included for the two classifications of burnup credit. These classes of burnup credit and the nuclides included within each are defined here for the purposes of analysis and discussion; other terminology and specific sets of nuclides have been defined and used by others studying the burnup credit phenomena. Note, however, that these studies are not sensitive to minor variations in the selection of nuclides within each class of burnup credit.

TABLE I  
Nuclides Associated with the Classifications of Burnup Credit Used for Analysis

| Actinide-Only Burnup Credit Nuclides                       |  |   |   |   |   |   |   |  |  |
|--|--|---|---|---|---|---|---|--|--|
| <sup>234</sup> U<br><sup>241</sup> Am                      | <sup>235</sup> U<br>O <sup>a</sup>                         | <sup>236</sup> U  | <sup>238</sup> U  | <sup>238</sup> Pu   | <sup>239</sup> Pu   | <sup>240</sup> Pu   | <sup>241</sup> Pu   | <sup>242</sup> Pu  | <sup>237</sup> Np                      |
| Actinide + Fission Product Burnup Credit Nuclides          |  |   |   |   |   |   |   |  |  |
| <sup>234</sup> U<br><sup>241</sup> Am<br><sup>150</sup> Sm | <sup>235</sup> U<br><sup>243</sup> Am<br><sup>151</sup> Sm | <sup>236</sup> U<br><sup>95</sup> Mo<br><sup>152</sup> Sm | <sup>238</sup> U<br><sup>99</sup> Tc<br><sup>143</sup> Nd | <sup>238</sup> Pu<br><sup>101</sup> Ru<br><sup>145</sup> Nd | <sup>239</sup> Pu<br><sup>103</sup> Rh<br><sup>151</sup> Eu | <sup>240</sup> Pu<br><sup>109</sup> Ag<br><sup>153</sup> Eu | <sup>241</sup> Pu<br><sup>133</sup> Cs<br><sup>155</sup> Gd | <sup>242</sup> Pu<br><sup>147</sup> Sm<br>O <sup>a</sup> | <sup>237</sup> Np<br><sup>149</sup> Sm |

<sup>a</sup>Oxygen is neither an actinide nor a fission product but is included in this list because it is an integral and important part of the fuel and thus is included in the calculations.

As there are many important variables in a burnup credit calculation (e.g., geometric configuration, nuclides included, cooling time, etc.), calculations to support this investigation include many variations. As it is acknowledged that confusion may arise regarding calculational models and assumptions when considering the numerous studies described in the following sections, Table II provides a summary of the various calculational models, identifies the specific sections within this paper that utilize each model, and notes exceptions where appropriate.

The analyses were performed from an away-from-reactor criticality safety perspective, which is concerned with the determination and usage of limiting configurations and conditions that encompass or bound the variety of anticipated configurations and conditions. For each unique fixed absorber design considered, a depletion calculation was performed for (a) the un-poisoned or uncontrolled assembly condition (i.e., no IBAs, BPRs, or CRs present) and (b) conditions in which the IBAs, BPRs, or CRs were assumed to be present for various periods of burnup. The calculated isotopic compositions from these conditions were subsequently used in criticality calculations for an out-of-reactor environment. Throughout the following sections, the  $\Delta k$  values between these two conditions are reported to assess the effect of the fixed absorbers on the reactivity of SNF. Consistent with the physical conditions (i.e., IBAs cannot be physically separated from the fuel), residual IBA material is included in the out-of-reactor criticality calculations. In contrast, BPRs and CRs are separated from the fuel and

hence are not included in the out-of-reactor criticality calculations.

### III. ANALYSES FOR IBAs

Although numerous types of IBAs have been used in U.S. commercial nuclear fuel assembly designs, all of the widely used designs are similar in that they contain thermal neutron absorbing material as an integral nonremoval part of the assembly. Variations in the IBA material, composition, placement within rods, and rod configurations exist among current PWR fuel designs. These characteristics are varied in combination with the assembly initial fuel enrichment and core location to achieve core operating and fuel management objectives.

For PWR fuels without IBAs, reactivity decreases with burnup in a nearly linear fashion. In contrast, for PWR fuel assembly designs that make significant use of IBAs, reactivity actually increases as fuel burnup proceeds, reaches a maximum at a burnup where the IBA is nearly depleted and then decreases with burnup in a nearly linear fashion. For fuel assembly designs that make modest use of IBAs, reactivity may decrease with burnup slowly up to the point where the IBA is nearly depleted and then decrease with burnup in the same nearly linear manner. Fuel assemblies are typically designed such that the burnable absorber is effectively depleted in the first cycle, and as a result, the assembly reactivity typically peaks within this period of burnup. Calculated  $k_{inf}$  values as a function of burnup

TABLE II  
Summary of Criticality Models Used for the Analysis

|  | Criticality Models   |  |   |
|--|--|--|---|
| Code                                       | HELIOS   | KENO V.a   | KENO V.a                                  |
| Dimensionality                             | 2-D  | 3-D  | 3-D                                       |
| Geometric configuration                    | Infinite assembly array <sup>a</sup>   | GBC-32 cask  | GBC-32 cask                               |
| Axial burnup distribution                  | N/A <sup>b</sup>   | Not included   | Included <sup>c</sup>                     |
| Nuclides included                          | All <sup>d</sup>   | Various <sup>e</sup>                                       | Various <sup>e</sup>                      |
| Cooling time (yr)                          | Zero <sup>f</sup>  | Various  | Various                                   |
| Sections discussing results from the model | III.A, III.B, III.C, III.D, III.E.1, <sup>a</sup> III.E.2, <sup>f</sup> IV.A, IV.B, V.A, V.B, V.C, V.D | IV.C.1, <sup>g</sup> IV.C.3, <sup>g</sup> V.E <sup>h</sup> | III.E.3, <sup>h</sup> IV.C.2 <sup>g</sup> |

<sup>a</sup>Results in Section III.E.1 correspond to an infinite radial array of cask storage cells, based on the GBC-32 cask.

<sup>b</sup>Not applicable.

<sup>c</sup>Axial burnup distribution used corresponds to the bounding profile suggested in Ref. 13 for PWR fuel with average-assembly discharge burnup >30 GWd/tonne U.

<sup>d</sup>All nuclides available in the 45-group neutron cross-section library that is distributed as part of the HELIOS-1.6 code package.<sup>9</sup>

<sup>e</sup>Calculations were performed with subsets of the available nuclides, as defined in Table I.

<sup>f</sup>Results discussed in Sec. III.E.2 correspond to various cooling times between zero and 40 yr.

<sup>g</sup>Results correspond to 5-yr cooling time.

<sup>h</sup>Results correspond to zero cooling time.

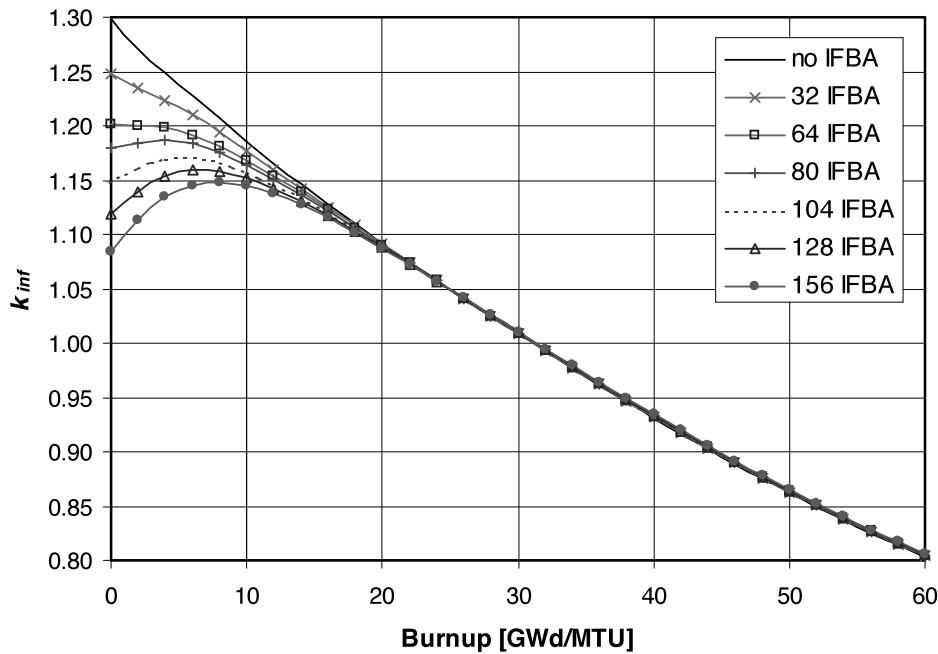


Fig. 1. Calculated  $k_{inf}$  as a function of burnup for PWR fuel with and without IBAs present. Legend indicates the number of IBA (IFBA) rods present in each case.

for PWR fuel with and without IBAs present are shown in Fig. 1 (using IFBA rods).

The presence of IBAs during depletion hardens the neutron spectrum, resulting in greater production of fissionable plutonium isotopes and reduced  $^{235}\text{U}$  depletion. Consequently, the reactivity of an assembly depleted with IBAs may be higher than that of an assembly depleted without IBAs. However, because assemblies are designed so that the IBA is effectively depleted in the first cycle, the assembly is exposed to a hardened spectrum during the first cycle of burnup only. Note that, unlike BPRs, CRs, and APSRs, which are inserted into assembly guide tubes, IBAs do not displace moderator in the assembly lattice and thus have a less significant impact on the neutron spectrum.

The following subsections describe the various IBA types and summarize detailed analyses to demonstrate the reactivity effect of IBAs as a function of burnup. Analyses have been performed for Westinghouse assembly designs with IFBAs, Combustion Engineering (CE) and Siemens assembly designs with  $\text{UO}_2\text{-Gd}_2\text{O}_3$  rods, CE assembly designs with  $\text{UO}_2\text{-Er}_2\text{O}_3$  rods, and CE assembly designs with  $\text{B}_4\text{C}$  rods. To the extent possible, analyses have been performed for a representative range of fuel initial enrichment and poison loading combinations based on actual plant data.

### III.A. IFBA Rods

Some Westinghouse fuel assembly designs include IFBA rods, which contain  $\text{UO}_2$  fuel pellets with a thin

coating of zirconium diboride ( $\text{ZrB}_2$ ) on the outer surface. Specification of the assembly designs that utilize IFBA rods include the boron loading in the  $\text{ZrB}_2$  coating, the number of IFBA rods, and the placement or loading pattern of the IFBA rods within the assembly. The number of IFBA rods within a fuel assembly may vary from zero to  $\sim 60\%$  of the total number of fuel rods. For a Westinghouse  $17 \times 17$  assembly, which contains 264 fuel rods, loading patterns with 0 (no IFBA), 8, 16, 32, 48, 64, 80, 104, 128, and 156 IFBA rods are known to exist. In addition, the boron loading in the  $\text{ZrB}_2$  coating and the initial  $^{235}\text{U}$  enrichment are varied to meet core management objectives.

Figure 1 shows  $k_{inf}$  values as a function of burnup for Westinghouse  $17 \times 17$  assemblies with 4.0 wt%  $^{235}\text{U}$  initial enrichment and varying numbers of IFBA rods with 0.618 mg  $^{10}\text{B}/\text{cm}$  (1.57 mg  $^{10}\text{B}/\text{in.}$ ) The differences in the  $k_{inf}$  values ( $\Delta k$  values) between cases with IFBA rods and the reference case without IFBA rods are plotted as a function of burnup in Fig. 2, where it is apparent that the  $\Delta k$  values become positive after the point at which the boron is essentially depleted. In other words, SNF assemblies that contain IFBA rods are slightly more reactive (positive  $\Delta k$ ) at discharge than assemblies without IFBA rods. Furthermore, the maximum positive  $\Delta k$  value increases with increasing numbers of IFBA rods and increasing poison loading (i.e.,  $^{10}\text{B}$  loading in the  $\text{ZrB}_2$ ). For a fixed number of IFBA rods, the maximum positive  $\Delta k$  value increases slightly with decreasing initial fuel enrichment. This behavior is shown in Fig. 3, which plots the  $\Delta k$  values between cases with 104

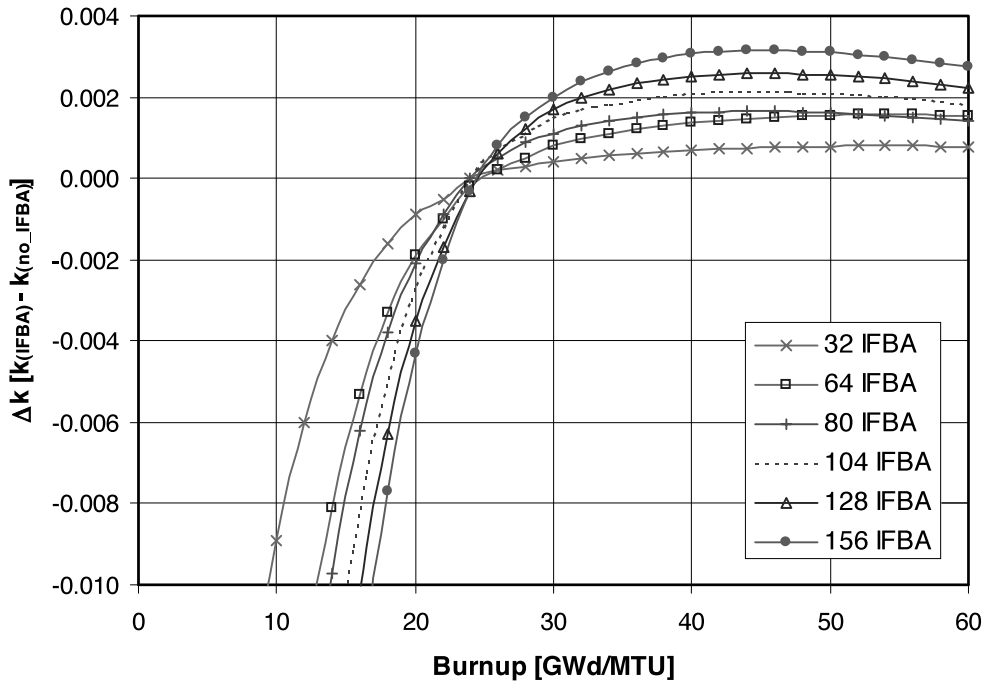


Fig. 2. Comparison of  $\Delta k$  values, as a function of burnup, between assemblies with and without IFBA rods present. Results correspond to Westinghouse  $17 \times 17$  assemblies with 4.0 wt%  $^{235}\text{U}$  initial enrichment.

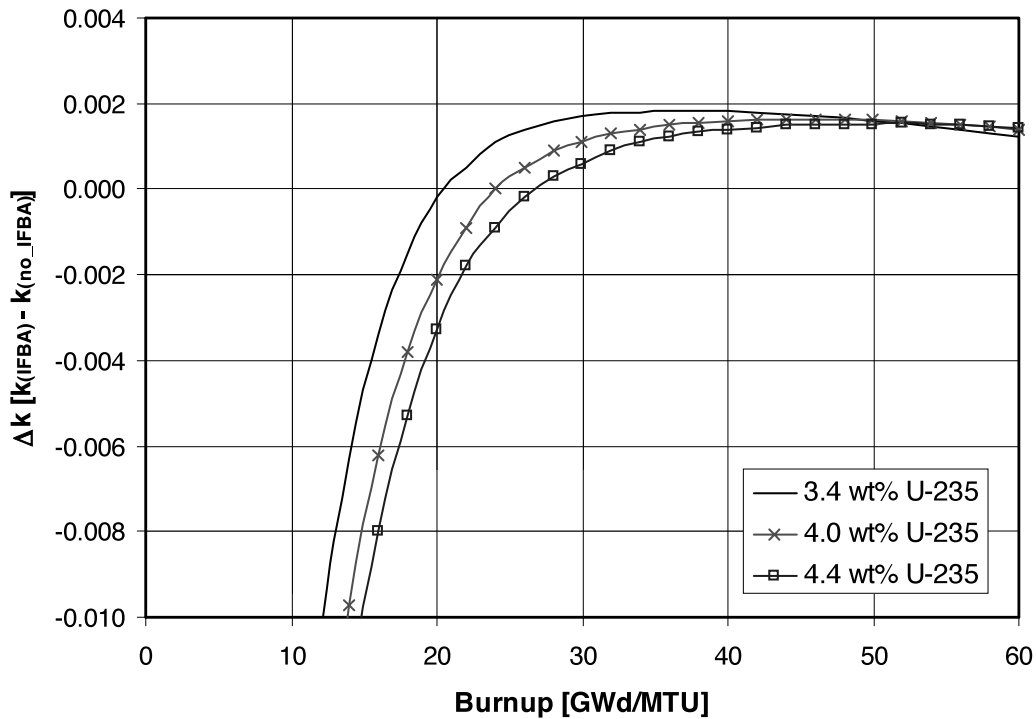


Fig. 3. Comparison of  $\Delta k$  values for varying initial enrichments between assemblies with and without IFBA rods present. Results correspond to Westinghouse  $17 \times 17$  assemblies; IFBA cases have 104 IFBA rods present.

TABLE III  
Specifications for Siemens 17 × 17 Fuel Assemblies with UO<sub>2</sub>-Gd<sub>2</sub>O<sub>3</sub> Fuel Rods

| Fuel Assembly Designator | UO <sub>2</sub> Fuel Rod Enrichment | Number of UO <sub>2</sub> Fuel Rods | Number of UO <sub>2</sub> -Gd <sub>2</sub> O <sub>3</sub> Rods | Gd <sub>2</sub> O <sub>3</sub> / <sup>235</sup> U wt% for UO <sub>2</sub> -Gd <sub>2</sub> O <sub>3</sub> Rods |
|--------------------------|-------------------------------------|-------------------------------------|--|--|
| S1                       | 4.25                                | 260                                 | 4  | 2.00/4.16 <sup>a</sup>   |
| S2                       | 4.25                                | 244                                 | 16<br>4  | 6.00/3.99<br>2.00/4.16   |
| S3                       | 4.25                                | 240                                 | 16<br>8  | 8.00/3.91<br>4.00/4.08   |
| S4                       | 4.25                                | 236                                 | 16<br>12   | 8.00/3.91<br>4.00/4.08   |

<sup>a</sup>Read as 2.0 wt% Gd<sub>2</sub>O<sub>3</sub> and 4.16 wt% <sup>235</sup>U in UO<sub>2</sub>-Gd<sub>2</sub>O<sub>3</sub> rods.

IFBA rods and reference cases without IFBA rods for varying initial enrichments.

Based on actual plant fuel data,<sup>15,16</sup> analyses were performed for variations in the initial fuel enrichment, the numbers of IFBA rods, and the <sup>10</sup>B loading in the IFBA rods within their respective ranges. The maximum positive  $\Delta k$  value was found to be 0.004, which corresponded to the maximum <sup>10</sup>B loading [0.9272 mg <sup>10</sup>B/cm (2.355 mg <sup>10</sup>B/in.)] and maximum number of IFBA rods (i.e., 156), for an initial enrichment of 4.617 wt% <sup>235</sup>U.

### III.B. UO<sub>2</sub>-Gd<sub>2</sub>O<sub>3</sub> Rods

A number of fuel vendors, including CE, Babcock & Wilcox (B&W), and Siemens,<sup>a</sup> have manufactured and used gadolinia-uranium (UO<sub>2</sub>-Gd<sub>2</sub>O<sub>3</sub>) IBA rods. These UO<sub>2</sub>-Gd<sub>2</sub>O<sub>3</sub> rods, or gadolinia rods, are fuel rods with gadolinia (Gd<sub>2</sub>O<sub>3</sub>) as an integral part of the fuel matrix and are also used extensively in boiling water reactors (BWRs). In comparison to normal UO<sub>2</sub> fuel rods, the use of gadolinia rods has the following known inherent penalties<sup>17</sup>:

1. Gadolinia displaces uranium in the fuel matrix, which results in a reduced heavy metal mass.
2. Due to the lower heat conductivity of the UO<sub>2</sub>-Gd<sub>2</sub>O<sub>3</sub> fuel, as compared to normal UO<sub>2</sub> fuel, the <sup>235</sup>U enrichment in the UO<sub>2</sub>-Gd<sub>2</sub>O<sub>3</sub> fuel rods is often reduced to meet the design criterion for maximum fuel temperature.
3. Following the depletion of the main neutron absorbing gadolinium isotopes (i.e., <sup>155</sup>Gd and <sup>157</sup>Gd), a residual negative reactivity remains due to the presence of gadolinium isotopes that are not destroyed.

The weight percent or loading of Gd<sub>2</sub>O<sub>3</sub> and the <sup>235</sup>U enrichment in gadolinia-bearing fuel rods are vari-

able. Further, the number of gadolinia-bearing fuel rods within an assembly is variable. Hence, various gadolinia loadings (weight percent of Gd<sub>2</sub>O<sub>3</sub> and number of gadolinia-bearing fuel rods) and initial fuel enrichment combinations were studied to establish the reactivity effect as a function of burnup. The combinations considered were based on actual fuel assemblies and were selected to encompass the range of known variations. Because CE assemblies include oversized water holes, while others (i.e., Siemens and B&W) do not, analyses were performed for both CE 16 × 16 and Siemens 17 × 17 fuel designs. Relevant specifications for four Siemens assembly designs considered are listed in Table III in order of increasing gadolinia inventory.

Figure 4 shows  $k_{inf}$  values as a function of burnup for each of the assemblies listed in Table III. Calculations were also performed for reference (unpoisoned) cases in which each of the UO<sub>2</sub>-Gd<sub>2</sub>O<sub>3</sub> fuel rods was replaced by an equivalent enrichment fuel rod without Gd<sub>2</sub>O<sub>3</sub>. Due to the variations in fuel rod enrichment, each of the assembly designs listed in Table III required a separate reference case. Differences in the  $k_{inf}$  values ( $\Delta k$  values) between cases with and without the Gd<sub>2</sub>O<sub>3</sub> present, for each of the four Siemens assembly designs, are shown in Fig. 5. The negative  $\Delta k$  values in Fig. 5 indicate that the gadolinia-bearing fuel is less reactive than the fuel without gadolinia. The extent by which the gadolinia-bearing fuel is always less reactive is seen to increase with increasing gadolinia loading (weight percent of Gd<sub>2</sub>O<sub>3</sub> and the number of gadolinia-bearing rods). Parametric analyses found that the  $\Delta k$  values are relatively insensitive to initial fuel enrichment.<sup>6</sup> Analyses were also performed for various gadolinia loading and initial enrichment combinations in CE 16 × 16 assemblies,<sup>18</sup> which include oversized water holes, and the results were consistent with those shown for the Siemens assemblies.<sup>6</sup> Therefore, we expect similar consistent results for fuel assemblies from the other fuel vendors since they have similar lattice arrangements.

<sup>a</sup>Although B&W and Siemens are now part of Framatome ANP, and thus no longer exist as separate entities, the names are used herein for consistency with the available fuel data.

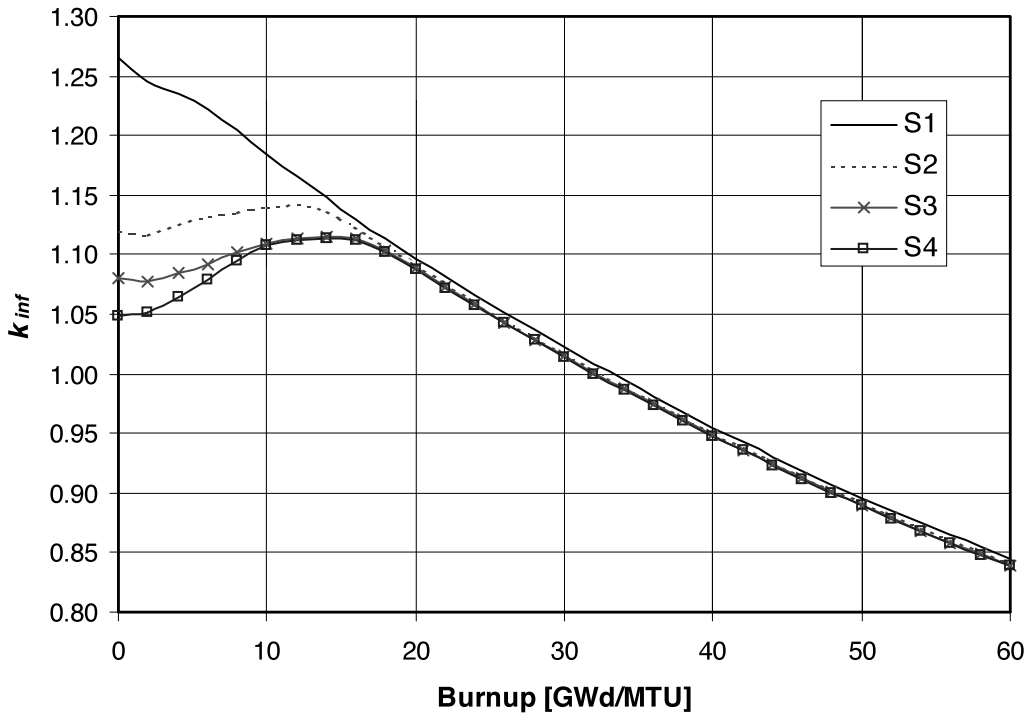


Fig. 4. Calculated  $k_{inf}$  as a function of burnup for PWR fuel with and without  $UO_2$ - $Gd_2O_3$  rods present. Legend indicates the fuel assembly designators that are described in Table III.

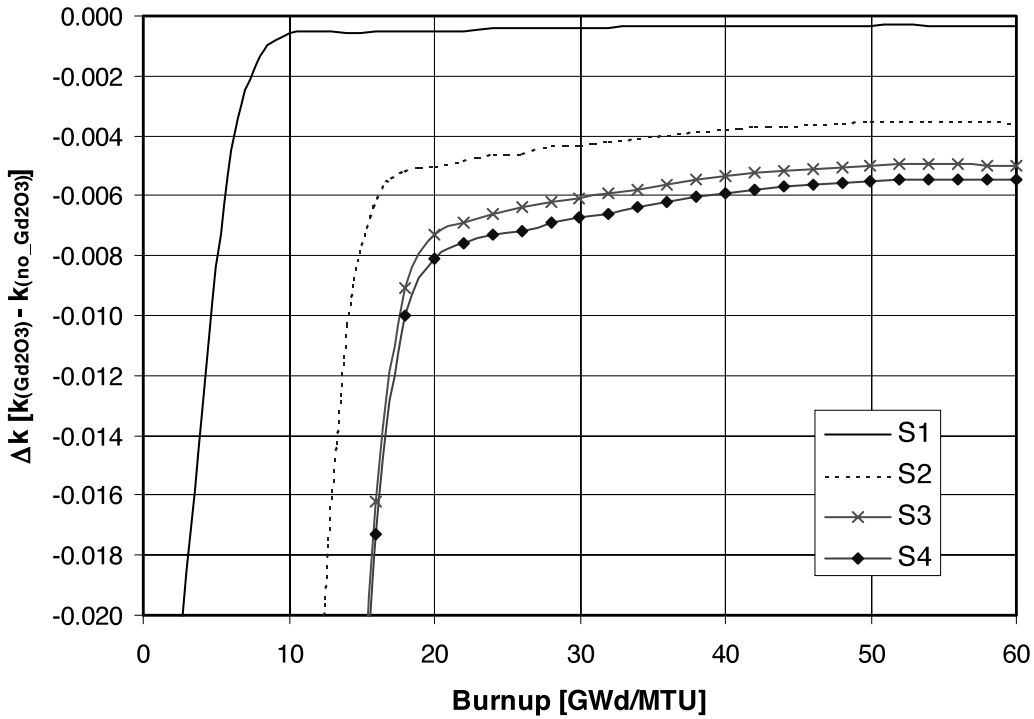


Fig. 5. Comparison of  $\Delta k$  values as a function of burnup between assemblies with and without  $UO_2$ - $Gd_2O_3$  rods present. Legend indicates the fuel assembly designators that are described in Table III.

While it is obvious that the reactivity early in burnup is decreased with increased poison (gadolinia) loading, it may not be immediately apparent why the behavior remains after the majority of the poison is depleted, especially considering that in Sec. III.A, increased IFBA loadings were shown to produce increased positive  $\Delta k$  values late in burnup. The reason for the persistence of lower  $\Delta k$  values with increasing gadolinia is related to the negative residual reactivity associated with the presence of the remaining minor gadolinium isotopes. Increased gadolinia loading leads to increased concentrations of the gadolinium isotopes, including the isotopes that are not significant neutron absorbers, and a corresponding decrease in the mass of uranium by simple displacement. Because these minor gadolinium isotopes are not significant neutron absorbers, their reactivity worth (due to their displacement of uranium) is relatively constant with burnup. As a result, the negative residual reactivity increases with gadolinia loading and more than offsets any positive reactivity influence due to the harder neutron spectrum associated with the presence of the gadolinia. In support of this discussion, Fig. 6 shows the reactivity worth of all of the gadolinium isotopes and the minor gadolinium isotopes ( $^{152}\text{Gd}$ ,  $^{154}\text{Gd}$ ,  $^{156}\text{Gd}$ ,  $^{158}\text{Gd}$ , and  $^{160}\text{Gd}$ ) as a function of burnup, and it shows how the negative residual reactivity increases with increasing gadolinia loading.

In contrast to the characteristics just described for gadolinia-bearing fuel, the  $\text{ZrB}_2$  coating on the IFBA fuel pellets does not displace uranium and thus does not

have any significant negative residual reactivity. Consequently, the positive reactivity influence, due to the harder neutron spectrum associated with the presence of the  $^{10}\text{B}$ , is not offset. Thus, as shown in Sec. III.A, the positive reactivity effect for IFBAs increases with increasing poison loading, either through increased  $^{10}\text{B}$  loading in the  $\text{ZrB}_2$  or increased number of IFBA rods.

### III.C. $\text{UO}_2\text{-Er}_2\text{O}_3$ Rods

In addition to  $\text{UO}_2\text{-Gd}_2\text{O}_3$  rods, CE has manufactured an IBA rod containing erbia ( $\text{Er}_2\text{O}_3$ ) for use with both  $14 \times 14$  and  $16 \times 16$  fuel assembly designs.<sup>16,19</sup> Similar to the  $\text{UO}_2\text{-Gd}_2\text{O}_3$  rods, the erbia rods include the burnable absorber  $\text{Er}_2\text{O}_3$  as an integral part of the fuel matrix, and the weight percent of the erbia and the number of erbia rods within an assembly are both variable, as well as the  $^{235}\text{U}$  enrichment. As a result, in comparison to normal  $\text{UO}_2$  fuel rods, the use of erbia rods has the same known inherent penalties that were identified previously for gadolinia rods.

Because erbia is not used as widely as other burnable absorbers (e.g.,  $^{10}\text{B}$  in IFBA or gadolinia), the design variations are more limited. To establish the reactivity effect of erbia rods, calculations were performed for erbia loadings (weight percent of  $\text{Er}_2\text{O}_3$  and number of erbia-bearing fuel rods) and initial fuel enrichment combinations that were selected to encompass the range of known variations, based on actual fuel assemblies. Figure 7 shows  $k_{inf}$  values as a function of burnup for the

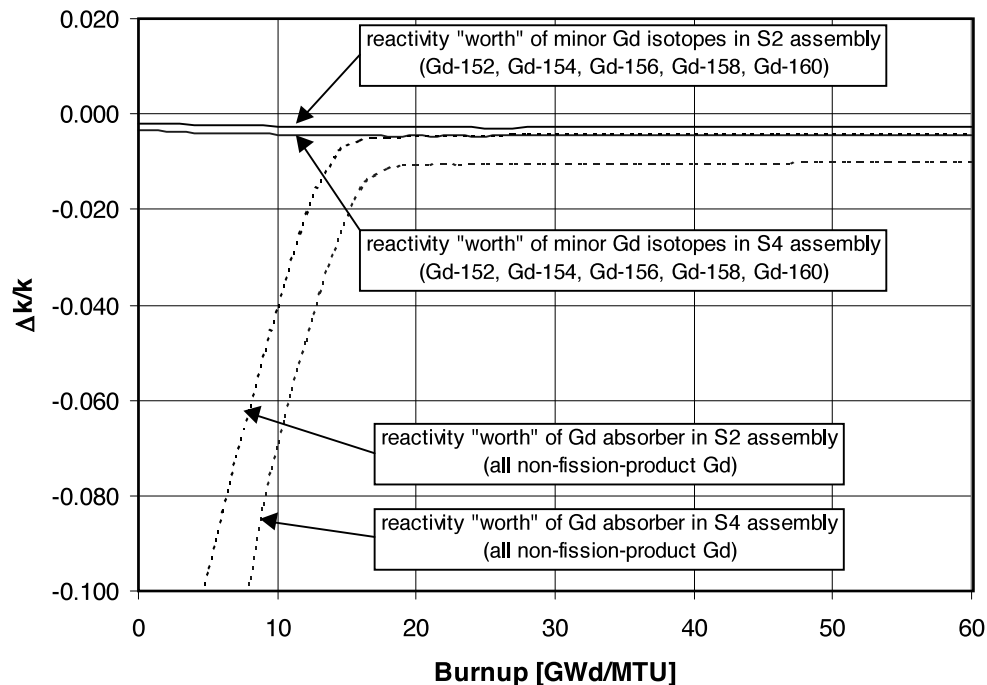


Fig. 6. Reactivity worth of gadolinium as a function of burnup for S2 and S4 assemblies (see Table III for assembly descriptions).

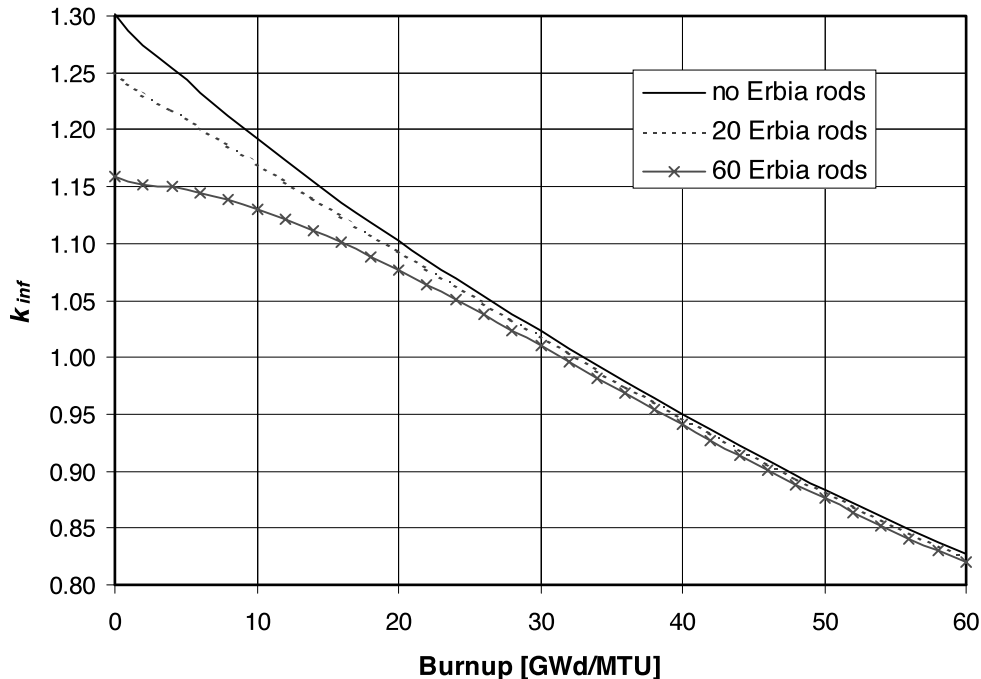


Fig. 7. Calculated  $k_{inf}$  as a function of burnup for PWR fuel with and without  $\text{UO}_2\text{-Er}_2\text{O}_3$  (2.0 wt%  $\text{Er}_2\text{O}_3$ ) rods present. Results correspond to CE  $14 \times 14$  assemblies with 4.3 wt%  $^{235}\text{U}$  initial enrichment; legend indicates the number of  $\text{UO}_2\text{-Er}_2\text{O}_3$  rods present in each case.

CE assemblies with various numbers of erbia-bearing rods present. The results corresponded to the CE  $14 \times 14$  assembly design with 4.3 wt%  $^{235}\text{U}$  initial enrichment and erbia-bearing rods with 2.0 wt%  $\text{Er}_2\text{O}_3$ . For the case without erbia-bearing rods, the erbia-bearing fuel rods were replaced by equivalent enrichment (4.3 wt%  $^{235}\text{U}$ ) fuel rods without erbia. Differences in the  $k_{inf}$  values ( $\Delta k$  values) between cases with and without the  $\text{Er}_2\text{O}_3$  present are shown in Fig. 8. Similar to the results shown for gadolinia-bearing fuel, the negative  $\Delta k$  values in Fig. 8 indicate that the erbia-bearing fuel is less reactive than the nonerbia-bearing fuel. In other words, erbia also has an associated negative residual reactivity. The extent by which the erbia-bearing fuel is less reactive increases with increasing erbia loading (weight percent of  $\text{Er}_2\text{O}_3$  and the number of erbia-bearing rods).

### III.D. $\text{Al}_2\text{O}_3\text{-B}_4\text{C}$ Rods

Another IBA manufactured by CE consists of solid rods containing alumina pellets with uniformly dispersed boron carbide particles ( $\text{Al}_2\text{O}_3\text{-B}_4\text{C}$ ) clad in Zircaloy. These  $\text{Al}_2\text{O}_3\text{-B}_4\text{C}$  rods have been used with both  $14 \times 14$  and  $16 \times 16$  fuel assembly designs. The weight percent of  $\text{B}_4\text{C}$  and the number of rods per assembly are variable. Unlike the IFBA,  $\text{UO}_2\text{-Gd}_2\text{O}_3$ , and  $\text{UO}_2\text{-Er}_2\text{O}_3$ , these rods do not contain fuel, and hence are actually referred to as BPRs elsewhere.<sup>19</sup> The  $\text{Al}_2\text{O}_3\text{-B}_4\text{C}$  rods

are classified herein as IBAs because they replace fuel rods (i.e., are not inserted into guide tubes) and are an integral nonremoval part of the fuel assembly and thus, from a burnup-credit analysis standpoint, fit more appropriately within the IBA classification.

Because  $\text{Al}_2\text{O}_3\text{-B}_4\text{C}$  rods are not used as widely as other burnup absorbers, design specifications and variations are limited. Based on the available specifications,<sup>16,19</sup> calculations were performed for CE  $14 \times 14$  assemblies with 4.0 wt%  $^{235}\text{U}$  initial enrichment and various numbers of  $\text{Al}_2\text{O}_3\text{-B}_4\text{C}$  rods (4.0 wt%  $\text{B}_4\text{C}$ ). Figure 9 shows the  $k_{inf}$  values as a function of burnup for the CE assemblies with various numbers of  $\text{Al}_2\text{O}_3\text{-B}_4\text{C}$  rods present. For the reference case without  $\text{Al}_2\text{O}_3\text{-B}_4\text{C}$  rods, the  $\text{Al}_2\text{O}_3\text{-B}_4\text{C}$  rods were replaced by normal  $\text{UO}_2$  fuel rods with enrichment equivalent to the fueled rods (i.e., 4.0 wt%  $^{235}\text{U}$ ). The rationale for the definition of the reference case is related to the application for which this study is intended (i.e., burnup-credit analyses). For simplicity and generality, it is desirable to minimize the number of assembly lattices considered in the criticality safety evaluation. Therefore, if fully fueled assemblies are demonstrated to be more reactive than assemblies that contain  $\text{Al}_2\text{O}_3\text{-B}_4\text{C}$  rods, safety analyses that consider fully fueled assemblies can be used to bound assemblies that contain  $\text{Al}_2\text{O}_3\text{-B}_4\text{C}$  rods.

Differences in the  $k_{inf}$  values ( $\Delta k$  values) between cases with and without the  $\text{Al}_2\text{O}_3\text{-B}_4\text{C}$  rods present are

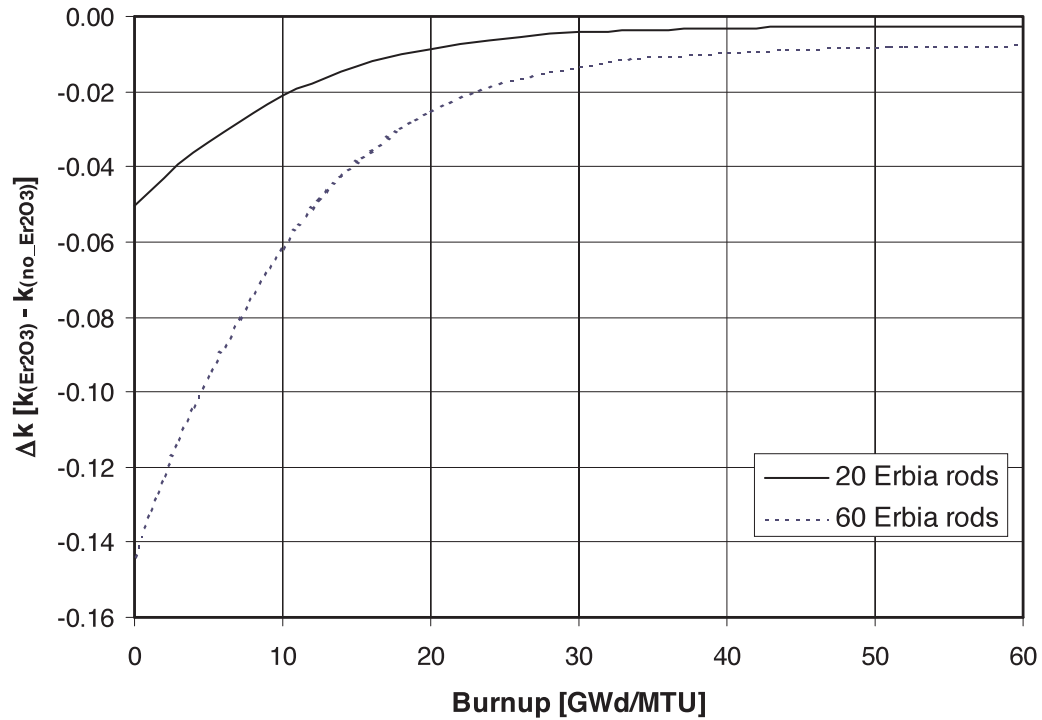


Fig. 8. Comparison of  $\Delta k$  values as a function of burnup between assemblies with and without  $\text{UO}_2\text{-Er}_2\text{O}_3$  (2.0 wt%  $\text{Er}_2\text{O}_3$ ) rods present. Legend indicates the number of  $\text{UO}_2\text{-Er}_2\text{O}_3$  rods present in each case.

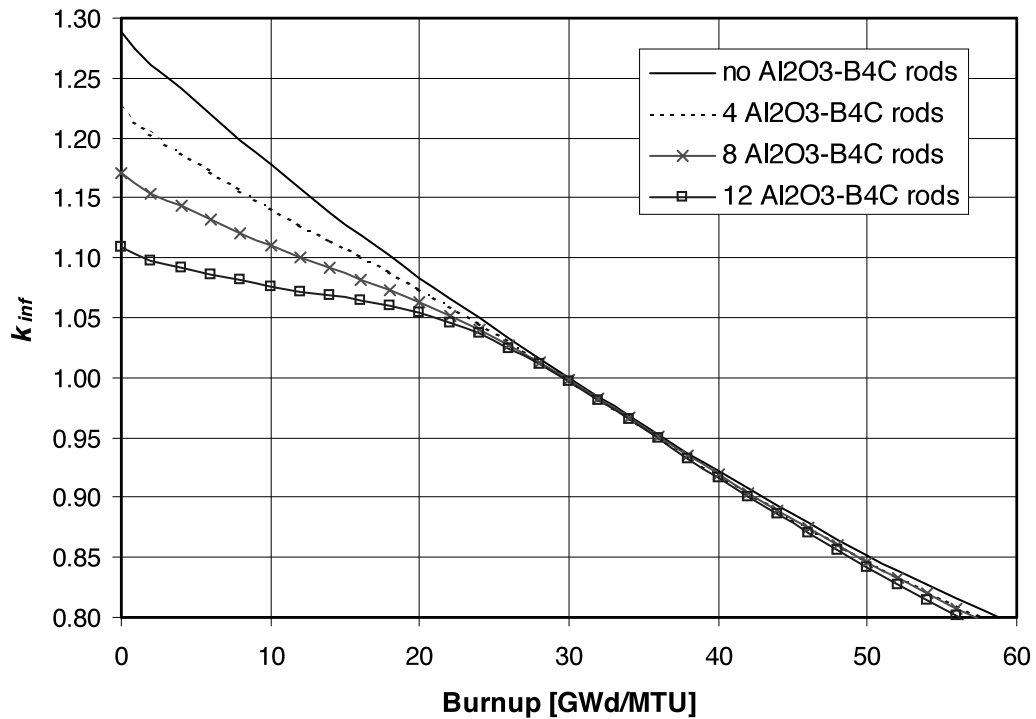


Fig. 9. Calculated  $k_{inf}$  as a function of burnup for PWR fuel with and without  $\text{Al}_2\text{O}_3\text{-B}_4\text{C}$  (4.0 wt%  $\text{B}_4\text{C}$ ) rods present. Results correspond to CE  $14 \times 14$  assemblies with 4.0 wt%  $^{235}\text{U}$  initial enrichment; legend indicates the number of  $\text{Al}_2\text{O}_3\text{-B}_4\text{C}$  rods present in each case.

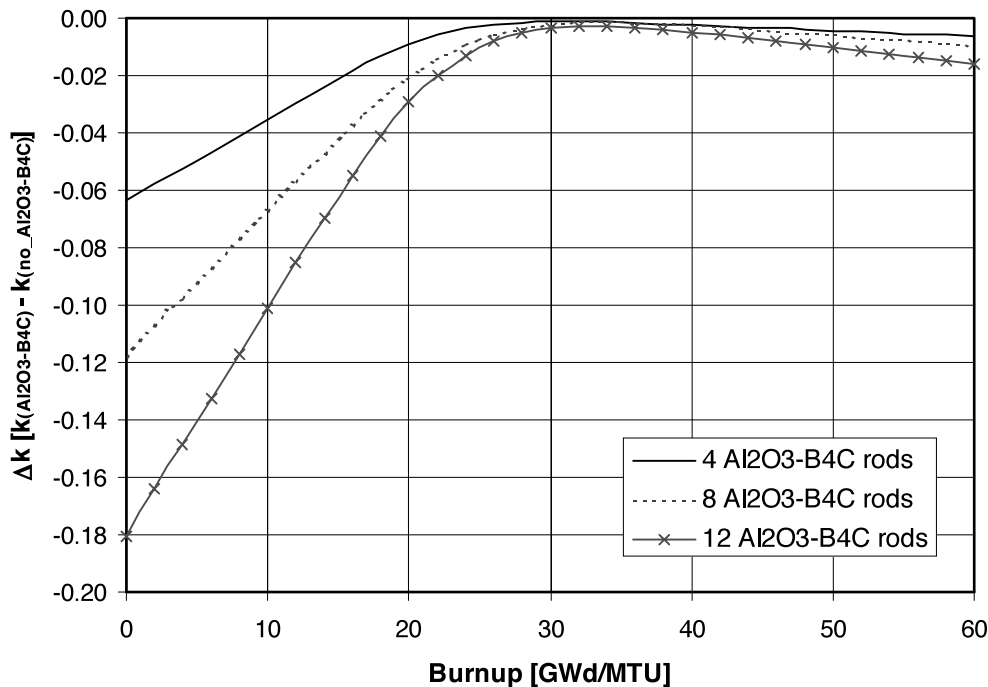


Fig. 10. Comparison of  $\Delta k$  values, as a function of burnup, between assemblies with and without  $\text{Al}_2\text{O}_3\text{-B}_4\text{C}$  (4.0 wt%  $\text{B}_4\text{C}$ ) rods present. Legend indicates the number of  $\text{Al}_2\text{O}_3\text{-B}_4\text{C}$  rods present in each case.

shown in Fig. 10, which confirms expectations that replacing fuel rods with  $\text{Al}_2\text{O}_3\text{-B}_4\text{C}$  rods results in a reduction in assembly reactivity. However, note that for the cases shown, which involve relatively few  $\text{Al}_2\text{O}_3\text{-B}_4\text{C}$  rods as compared to the total number of rod positions (176), the results show that the  $k_{inf}$  values with  $\text{Al}_2\text{O}_3\text{-B}_4\text{C}$  rods approach those of the reference case as the  $^{10}\text{B}$  is depleted.

### III.E. Additional Studies and Discussion

As this study was performed in support of burnup credit, a number of the aforementioned calculations were repeated with modeling assumptions and conditions associated with burnup-credit analyses to assess their impact on the results. In particular, the effect of cask geometry (presence of fixed absorber panels), cooling time, and the axial burnup distribution were studied for selected cases. These studies are discussed in the following sections.

#### III.E.1. Effect of Storage Cell Absorber Panels

The presence of fixed absorbers panels (e.g., Boral), which are commonly used in SNF cask storage cells, affects the neutron spectrum, and thus their presence can be an important consideration in burnup-credit analyses. This is particularly true when estimating the reactivity worth of thermal neutron absorbers (e.g., fission products), because the absorbers compete for neutrons with

the poison (e.g., boron) in the fixed absorber panels. For example, it has been shown in numerous studies (e.g., Refs. 5 and 14) that the reactivity worth of fission products is reduced by the presence of fixed absorber panels, as compared to estimates of the reactivity worth of fission products in a configuration without fixed absorber panels present (e.g., infinite pin lattice). To evaluate the impact of fixed absorbers, a number of the HELIOS calculations were repeated using an infinite array of poisoned storage cells from the GBC-32 cask, which is a generic 32-PWR assembly cask developed to be representative of actual burnup-credit casks designed by industry. A cross-sectional view of the GBC-32 cask is shown in Fig. 11. The boron loading in the Boral panels in the GBC-32 cask is  $0.0225 \text{ g } ^{10}\text{B}/\text{cm}^2$ ; detailed specifications for the GBC-32 cask are available in Ref. 20.

Although notable differences (inconsequential with respect to burnup credit) are observed for low burnups, where IBA poisons are still present in significant quantities and compete with the fixed absorber panels for thermal neutrons, the differences become very small at higher burnup as the IBA material is depleted. The behavior is illustrated in Figs. 12 and 13, which compare  $\Delta k$  values based on (a) infinite assembly array and (b) infinite poisoned storage cell array calculations for assemblies with IFBA and  $\text{UO}_2\text{-Gd}_2\text{O}_3$  rods, respectively. In general, the reactivity worth of the fixed absorber panels is lower for assemblies that have been depleted with IBAs than for assemblies without IBAs. Hence, the

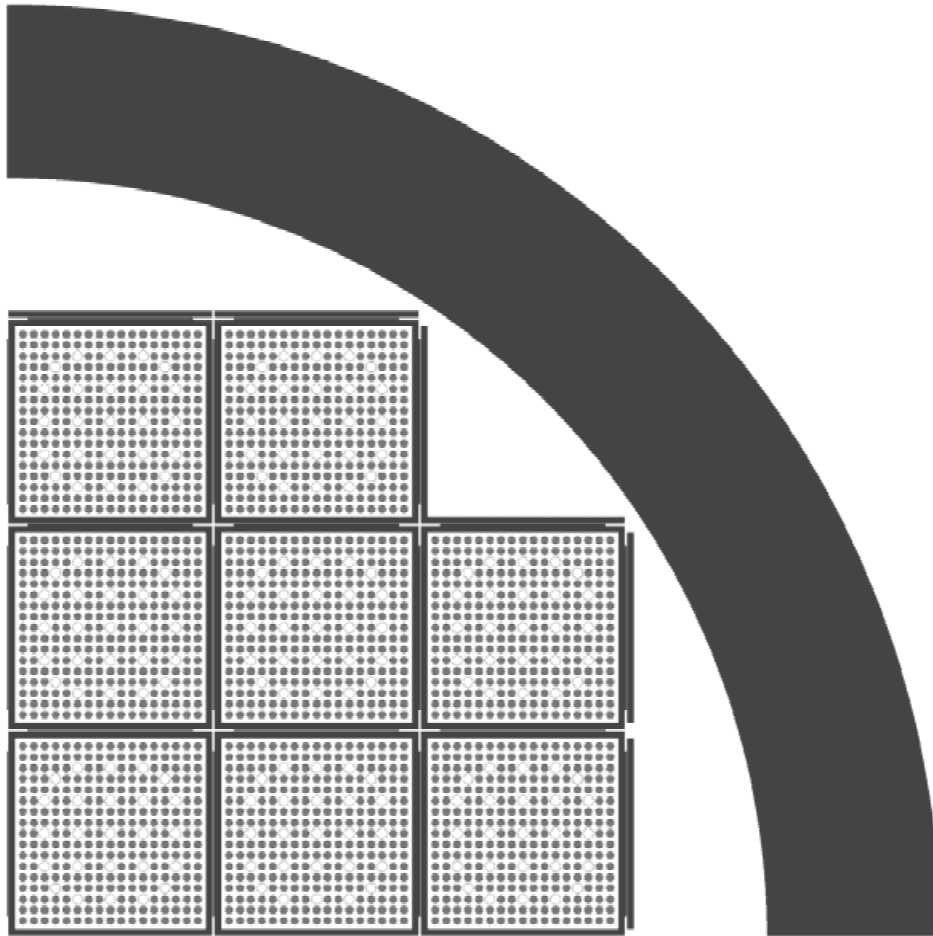


Fig. 11. Cross-sectional view of one quarter of the GBC-32 cask.

presence of the fixed absorber panels between assemblies tends to increase the  $\Delta k$  values with respect to the cases without fixed absorber panels. Most notably, the maximum positive  $\Delta k$  value associated with the IFBA cases was found to increase from 0.004 (for an infinite assembly array configuration) to 0.005 (for the poisoned cask storage cell configuration). However, the following conclusions, based on infinite assembly arrays remain valid:

1. The neutron multiplication factor for an assembly without IBAs is always greater (as a function of burnup) than the neutron multiplication factor for an assembly that utilized any of the following IBA types:  $\text{UO}_2\text{-Gd}_2\text{O}_3$ ,  $\text{UO}_2\text{-Er}_2\text{O}_3$ , or  $\text{Al}_2\text{O}_3\text{-B}_4\text{C}$  rods.

2. The neutron multiplication factor for an assembly with IFBA rods present was found to exceed (maximum of 0.5%  $\Delta k$ ) the neutron multiplication factor for an assembly without IFBA rods for burnup  $\geq 20$  GWd/tonne U.

The only exception that was found with the storage cell analyses was that the S1 case (see Table III), which

has an insignificant gadolinia loading (four  $\text{UO}_2\text{-Gd}_2\text{O}_3$  rods with 2.0 wt%  $\text{Gd}_2\text{O}_3$ ), yielded an insignificant positive reactivity effect ( $< 0.0005 \Delta k$ ). Increased gadolinia loadings result in increasing negative  $\Delta k$  values. Considering the unusually low gadolinia loading in the S1 case and the inconsequential  $\Delta k$  value, we do not consider this case to be important.

### III.E.2. Effect of Cooling Time

Cooling time is an important parameter in a burnup-credit evaluation. Numerous studies have shown (e.g., Ref. 21) that SNF discharged from a reactor will increase in reactivity for  $\sim 100$  h after discharge due to the decrease in neutron absorption caused by the decay of very short-lived fission products. The decrease in reactivity from 100 h to 100 yr is driven by the decay of the  $^{241}\text{Pu}$  fissile nuclide ( $t_{1/2} = 14.4$  yr) and the buildup of the neutron absorbers  $^{241}\text{Am}$  (from decay of  $^{241}\text{Pu}$ ) and  $^{155}\text{Gd}$  (from  $^{155}\text{Eu}$  which decays with  $t_{1/2} = 4.7$  yr). After  $\sim 50$  yr, the  $^{155}\text{Gd}$  buildup is complete, and the  $^{241}\text{Pu}$  has decayed out by  $\sim 100$  yr.

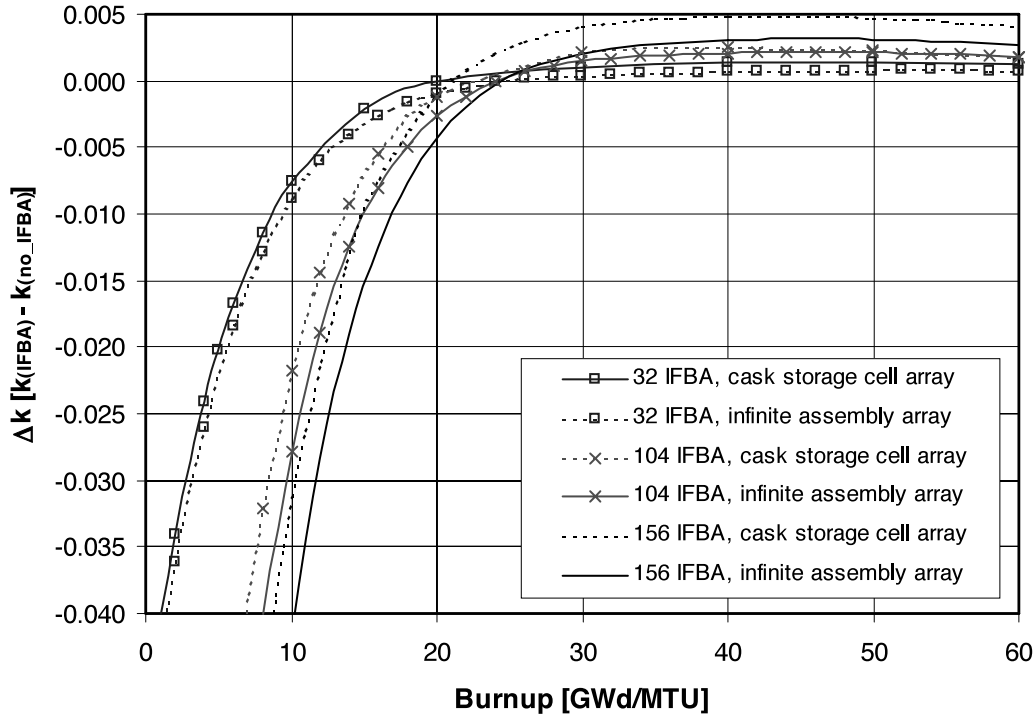


Fig. 12. Comparison of  $\Delta k$  values in a cask storage cell between assemblies with and without IFBA rods present. Results correspond to Westinghouse  $17 \times 17$  assemblies with 4.0 wt%  $^{235}\text{U}$  initial enrichment.

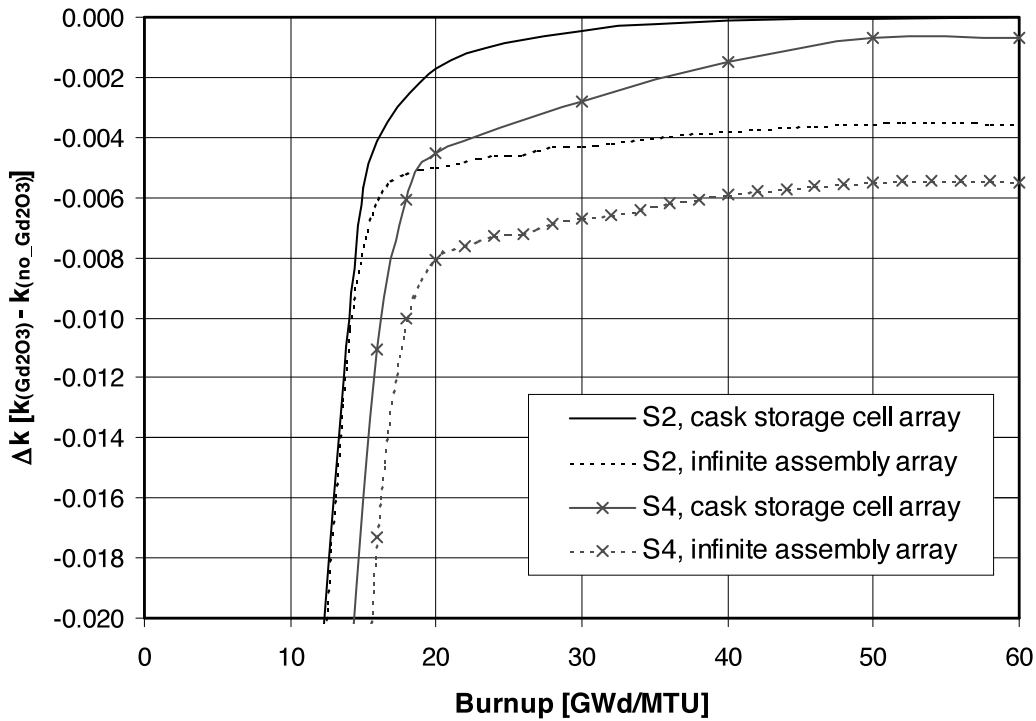


Fig. 13. Comparison of  $\Delta k$  values in a cask storage cell between assemblies with and without  $\text{UO}_2\text{-Gd}_2\text{O}_3$  rods present. Legend indicates the fuel assembly designators that are described in Table III.

After this time, the reactivity begins to increase, governed primarily by the decay of two major neutron absorbers— $^{241}\text{Am}$  ( $t_{1/2} = 432.7$  yr) and  $^{240}\text{Pu}$  ( $t_{1/2} = 6560$  yr)—and mitigated somewhat by a decrease in the fissile inventory as  $^{239}\text{Pu}$  ( $t_{1/2} = 24\,100$  yr) decays and causes an increase in  $^{235}\text{U}$ . After  $\sim 30\,000$  yr, the  $^{240}\text{Pu}$  and  $^{241}\text{Am}$  decay is complete, and the reactivity again begins to decrease as the decay of  $^{239}\text{Pu}$  dominates the process.

For simplicity, the aforementioned HELIOS analyses correspond to zero cooling time. To evaluate the effect of cooling time, HELIOS calculations were performed for selected cases (with and without absorber panels present) with cooling times more representative of cask storage and transportation (i.e., 5 to 40 yr). These calculations<sup>6</sup> showed that the  $\Delta k$  values between cases with and without IBAs were insensitive to cooling time, and thus the results at zero cooling time are expected to be applicable within the time frame relevant to cask storage and transportation.

### III.E.3. Effect of Axial Burnup Distribution

Numerous studies have been performed to investigate and quantify the reactivity effect associated with axial burnup distributions. A fairly comprehensive review of those studies is available in Ref. 22. In general, inclusion of the axial burnup distribution may result in an increase in the neutron multiplication factor for SNF, as compared to a uniform axial burnup modeling assumption, and thus is an important part of a burnup-credit analysis. The increase in reactivity is due to the underburned (with respect to the assembly-average burnup) regions near the fuel ends. With IBAs in a fuel assembly, the underburned end regions will have more residual absorber material present than the center region. Therefore, it was anticipated that the positive reactivity effect of the axial burnup distribution would actually be suppressed by the presence of IBAs. To evaluate this expectation, specific analyses were performed with an axial burnup distribution and included the residual IBA material.

For this study, 3-D criticality calculations were performed with the KENO V.a Monte Carlo code, using spent-fuel isotopics from HELIOS calculations. Note that only the primary actinide and fission products that have been previously determined to be important to burnup credit and the residual absorber material were included in the KENO V.a criticality model. These actinide and fission product nuclides are listed in Table I for reference. The GBC-32 burnup-credit cask and the Westinghouse  $17 \times 17$  assembly were used for this study. Because the IFBA rods were the only IBA type to yield a positive reactivity effect, they were used for this study.

A comparison was made between cases with no IFBA rods present and cases with 104 IFBA rods present, with a poison loading of  $0.618$  mg  $^{10}\text{B}/\text{cm}$  ( $1.57$  mg  $^{10}\text{B}/\text{in.}$ ). The IFBA coating was assumed to cover the entire active

fuel length [i.e.,  $365.76$  cm ( $144$  in.)]. The fuel in both cases had an initial enrichment of  $4.0$  wt%  $^{235}\text{U}$  and assembly-average burnups of  $15$ ,  $30$ ,  $45$ , and  $60$  GWd/tonne U were considered. The active fuel length of the assemblies was divided into 18 equal-length axial regions to model the variation in axial fuel and IBA composition associated with the burnup distribution. The axial burnup distribution used corresponds to the bounding profile suggested in Ref. 13 for PWR fuel with assembly-average discharge burnup  $>30$  GWd/tonne U.

As expected, for a typical initial enrichment and discharge burnup combination (i.e.,  $4.0$  wt%  $^{235}\text{U}$  and  $45$  GWd/tonne U), the case with IFBA rods yielded a slightly lower ( $\sim 0.005 \Delta k$ ) effective neutron multiplication factor  $k_{\text{eff}}$  than the case without IFBA rods present (both cases include the axial burnup distribution). This is due to the small residual IBA material in the underburned end regions, which dominate the neutron multiplication in the SNF. Additional comparisons shown in Table IV for both higher and lower assembly-average burnups confirm that the difference between cases with and without IFBAs decreases with burnup; for high burnups (e.g.,  $60$  GWd/tonne U) where the residual absorber in the end regions is essentially depleted, the difference is very small. Note that results are provided in Table IV for cases with and without fission products present and that the results are in good agreement.

A review of the relevant literature indicates that the IFBA coating seldom (if ever) extends over the entire active fuel length. Rather, the IFBA coating may vary in axial location and length. Therefore, additional calculations were performed for reduced IFBA coating lengths of  $304.8$  cm ( $120$  in.) and  $274.32$  cm ( $108$  in.), assuming the IFBA coating is centered with respect to the active fuel length. The results<sup>6</sup> show that for these shorter IFBA coating lengths, a case with IFBA rods can yield higher  $k_{\text{eff}}$  values than a corresponding case without IFBA rods. Further, the results show that as the IFBA coating length decreases, the difference ( $\Delta k$ ) between cases with and without IFBA rods present becomes positive earlier in burnup. This is because the underburned end regions have less residual IBA material due to the shorter IFBA coating length.

These results are important because they show that the effect of the IFBA rods (positive or negative) is dependent on the axial length of the IFBA coating; for typical IFBA coating lengths [e.g.,  $294.64$  cm ( $116$  in.) to  $340.36$  cm ( $134$  in.)], there is a small positive effect associated with the IFBA rods. Finally, the results support the expectation that assemblies with the other types of IBAs over the full axial length of the fuel are less reactive, as compared to assemblies without IBAs, than what was shown with the 2-D calculations.

### III.F. Summary of IBA Analyses

The results presented in this section are important to burnup credit because they demonstrate that

TABLE IV

Comparison of  $k_{eff}$  Results in the GBC-32 Cask for Fuel with IFBA Rods When the Axial Burnup Distribution Is Included

| Burnup<br>(GWd/tonne U)       | $k_{eff} \pm 1-\sigma$               |                                  | $\Delta k$<br>( $k_{IFBA} - k_{no\_IFBA}$ ) |
|-------------------------------|--------------------------------------|----------------------------------|---|
|                               | Reference Case<br>(no IFBAs present) | IFBA Case<br>(104 IFBAs present) |   |
| Actinide Only                 |                                      |                                  |   |
| 15                            | 1.0621 ± 0.0006                      | 1.0518 ± 0.0006                  | -0.0103 ± 0.0008                            |
| 30                            | 0.9933 ± 0.0006                      | 0.9844 ± 0.0005                  | -0.0089 ± 0.0008                            |
| 45                            | 0.9419 ± 0.0005                      | 0.9350 ± 0.0005                  | -0.0069 ± 0.0007                            |
| 60                            | 0.8959 ± 0.0006                      | 0.8934 ± 0.0006                  | -0.0025 ± 0.0008                            |
| Actinide and Fission Products |                                      |                                  |   |
| 15                            | 1.0235 ± 0.0006                      | 1.0137 ± 0.0005                  | -0.0098 ± 0.0008                            |
| 30                            | 0.9406 ± 0.0005                      | 0.9336 ± 0.0006                  | -0.0070 ± 0.0008                            |
| 45                            | 0.8782 ± 0.0006                      | 0.8729 ± 0.0006                  | -0.0053 ± 0.0009                            |
| 60                            | 0.8223 ± 0.0007                      | 0.8209 ± 0.0007                  | -0.0014 ± 0.0010                            |

assembly designs with  $UO_2-Gd_2O_3$ ,  $UO_2-Er_2O_3$ , or  $Al_2O_3-B_4C$  IBA rods are less reactive throughout burnup than their corresponding designs without the IBA rods (i.e., nonpoisoned, equivalent enrichment). Consequently, with the exception of assemblies with IFBA rods, neglecting the presence of IBAs in a burnup-credit criticality safety evaluation will yield slightly conservative results. These results are consistent with previous work,<sup>23</sup> which provided illustrative examples of the reactivity effects of several of the IBA types based on a 2-D analysis of a single case for each type. Considering the variations in IBA assembly designs, neglecting the presence of IBAs is an important simplifying assumption that does not add significant unnecessary conservatism.

For assembly designs with IFBA rods, 2-D calculations have demonstrated that the neutron multiplication factor is slightly greater (maximum of ~0.5%  $\Delta k$ ) than the neutron multiplication factor for assembly designs without IFBA rods. Three-dimensional cask calculations showed that when the axial burnup distribution is included, assemblies with full axial length IFBA coatings are less reactive than corresponding assemblies without IFBA rods because of the residual absorber present in the underburned end regions. However, the results also indicated that the effect of the IFBA rods is dependent on the axial length of the poison coating and that for typical IFBA coating lengths, there is a small positive effect associated with the IFBA rods. Consequently, the positive reactivity effect due to the presence of IFBA rods should be considered in any burnup-credit criticality safety analysis seeking to qualify IFBA assemblies as acceptable contents.

The analyses provide a technical basis for burnup credit with assembly designs that use IBAs. Although the analyses do not address the issue of validation of depletion methods for assembly designs with IBAs, they do demonstrate that the effect of the IBAs is relatively small and generally well behaved. Burnable absorber normalized atom densities are shown in Fig. 14 to highlight the differences in the depletion rates between the various burnable absorber materials.

#### IV. ANALYSES FOR BPRs

Three different BPR designs have been primarily used in U.S. commercial nuclear PWRs. The designs are all similar in that they contain thermal neutron absorbing material (boron) in rods sized to fit within fuel assembly guide tubes. Burnable poison rod assemblies (BPRAs) consist of a finite number and configuration of BPRs to be inserted into a PWR fuel assembly. The BPR characteristics (e.g., BPR number, configuration, and poison loading) may be varied in combination with the fuel assembly initial enrichment and core location to achieve core operating and fuel management objectives.

The presence of BPRs during depletion hardens the neutron spectrum due to removal of thermal neutrons by capture and by displacement of moderator, resulting in enhanced production of fissile plutonium isotopes and diminished  $^{235}U$  depletion. As a result, an assembly exposed to BPRs may have a higher reactivity for a given burnup than an assembly that has not used BPRs. Previous studies to assess the significance of BPRs for SNF

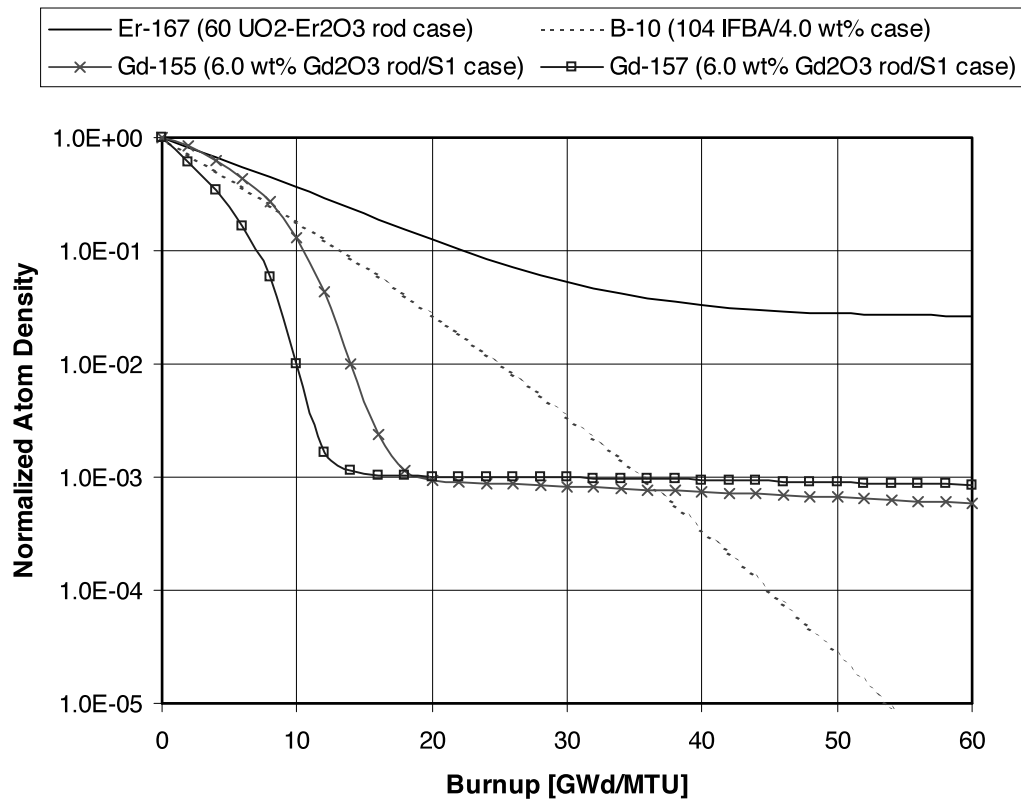


Fig. 14. Normalized atom densities as a function of burnup for the various IBA materials.

are minimal, but early work<sup>24</sup> for a single case concluded that insertion of maximum BPR loading in all depletion analyses would be a simple, yet not overly conservative approach to enable allowance for assemblies that have been exposed to BPRs.

The effect of BPRs on reactivity is dependent on the duration that the BPRs are present, the subsequent accumulated burnup, the BPR design, and the initial fuel assembly enrichment. Consequently, it is important to understand typical operating practices and variations in BPR designs. In U.S. PWR operations, BPRAs are typically inserted into a fuel assembly during its first cycle in the reactor core. Depending on the vendor, the number of BPRs within a BPRa (Westinghouse) or the poison loading in the BPRs within a BPRa (B&W) is variable. Based on limited Westinghouse plant operational data,<sup>24–28</sup> the average number of Westinghouse BPRs in a BPRa is typically much less than the maximum possible (dictated by the number of guide tubes in the assembly). For example, review of operational data in Refs. 26, 27, and 28 shows that the number of BPRs per BPRa, averaged over a core, is ~65% of the maximum possible. Therefore, for an assembly with 24 guide tubes, the average number of BPRs per BPRa is ~16. Similarly, based on limited B&W plant operational data,<sup>29</sup> the average poison loading (weight percent of B<sub>4</sub>C) in the BPRs is typically much less than the design maximum.

Due to the depletion of the neutron absorbing material (boron), BPRAs are typically (but not always) discarded after one-cycle residence in the core.<sup>24–28</sup> However, documented examples of the use of depleted BPRs are available.<sup>27,28</sup> Therefore, parametric analyses were performed for a variety of scenarios to establish an increased understanding and quantify the effect of BPR usage on the reactivity of discharged SNF. Trends in the reactivity effects of BPRs were established with infinite assembly array calculations. Subsequently, the reactivity effects of BPRs for typical initial enrichment and burnup combinations were quantified based on 3-D KENO V.a calculations with the GBC-32 cask.

Variations in BPR usage (i.e., duration of presence during burnup), BPR design characteristics, and initial fuel assembly enrichment were considered for all BPR designs that have been widely used in U.S. commercial PWRs. These include the Westinghouse Pyrex burnable absorber assembly (BAA), the Westinghouse wet annular burnable assembly (WABA), and the B&W BPR designs. For clarity, each of the BPR designs considered in this paper is described later in this section. The complete BPR design specifications required for this analysis are documented in Ref. 7. Note that the CE Al<sub>2</sub>O<sub>3</sub>-B<sub>4</sub>C rods considered in Sec. III are referred to elsewhere<sup>19</sup> as BPRs. However, unlike the Westinghouse and B&W BPR designs considered in this section, the CE Al<sub>2</sub>O<sub>3</sub>-B<sub>4</sub>C rods

may not be separated (withdrawn) from the assembly. Hence, they are classified herein as IBAs, and their impact on burnup-credit analyses is discussed in Sec. III.D.

#### IV.A. Westinghouse BPR Designs

Westinghouse has manufactured two main types of BPRs (Refs. 30 and 31): Pyrex BAAs and WABAs. The BAA BPRs utilize borosilicate glass ( $B_2O_3$ - $SiO_2$  with 12.5 wt%  $B_2O_3$ ) in the form of Pyrex tubing as a neutron absorber with a void central region.<sup>26</sup> The Pyrex BAA BPRs are clad in Type 304 stainless steel. WABA BPRs are similar to BAA BPRs but use annular pellets of  $Al_2O_3$ - $B_4C$  (14.0 wt%  $B_4C$ ) as the neutron absorber and have a wet (water-filled) central region.<sup>25</sup> The WABA BPRs are clad in Zircaloy. Configurations of BAA and WABA BPRs have been identified with varying (4 to 24) numbers of rods.<sup>30,31</sup>

For both Westinghouse BPR designs, depletion calculations were performed assuming the maximum possible number of BPRs present (i.e., 24) in a  $17 \times 17$  assembly. Calculations were also performed with fewer BPRs present to assess the effect as a function of the number of BPRs present. For the depletion calculations, three cycles of 15 GWd/tonne U per cycle were assumed. In general, calculations were performed assuming that the BPRs were present during (a) the first cycle of irradiation, (b) the first two cycles of irradiation, and (c) the entire irradiation period (i.e., all three cycles). For comparison purposes, reference calculations were performed assuming no BPRs present.

##### IV.A.1. Wet Annular Burnable Absorber BPRs

Figure 15 shows differences in the  $k_{inf}$  values ( $\Delta k$  values relative to the reference no BPR condition) as a function of burnup for initial fuel enrichments of 3.0, 4.0, and 5.0 wt%  $^{235}U$ , respectively. The results correspond to out-of-reactor conditions (i.e., unborated moderator at 20°C) and zero cooling time, and include all of the actinide and fission product nuclides available in the HELIOS cross-section library. It is evident from the figures that the reactivity effect of BPRs increases with increasing BPR exposure; thus, it is conservative (maximize reactivity) to assume that BPRs are present throughout the irradiation.

*IV.A.1.a. Effect of Initial Fuel Enrichment.* Figure 15 also demonstrates a decrease in the reactivity effect of BPRs with increasing initial fuel enrichment (for a fixed burnup). For initial enrichments of 3.0, 4.0, and 5.0 wt%  $^{235}U$ ,  $\Delta k$  values for continuous BPR exposure up to a burnup of 45 GWd/tonne U are 0.0194, 0.0155, and 0.0109, respectively. Note that fuel assemblies with initial enrichments of 3.0 wt%  $^{235}U$  do not typically achieve burnups as high as 45 GWd/tonne U. In practice, discharge burnups decrease with decreasing initial enrichment. Therefore, examination of a typical burnup and enrichment combination provides a reasonable rep-

resentation of the reactivity effect for other typical discharge burnup and enrichment combinations. As an example, compare the  $\Delta k$  values for 4.0 wt%  $^{235}U$  fuel burned to 45 GWd/tonne U (0.0155  $\Delta k$  from Fig. 15) and 3.0 wt%  $^{235}U$  fuel burned to 30 GWd/tonne U (0.0149  $\Delta k$  from Fig. 15).

Figure 15 includes the results of parametric analyses for a variety of exposure scenarios to establish an increased understanding of the effect of BPR exposure on the reactivity of discharged SNF; they do not all represent plausible realistic scenarios. Based on the authors' research of BPR usage in U.S. PWRs, BPRAs have been typically inserted into a fuel assembly during its first exposure cycle, which generally corresponds to somewhat more than one-third of its ultimate three-cycle burnup. In less frequent instances, BPRAs have been used in fuel assemblies during their second exposure cycle, either cumulative two-cycle exposure or isolated second-cycle exposure (i.e., no first-cycle exposure).<sup>24-26,28</sup> The effect of initial fuel enrichment on possible exposure conditions is shown in Fig. 15.

*IV.A.1.b. Effect of Variations in the Number of BPRs Present.* The Westinghouse BPRAs are composed of various numbers of BPRs arranged in specific geometric patterns. Although numerous patterns are known to exist,<sup>25</sup> including asymmetric arrangements, only symmetric assembly lattices were considered in this analysis. To demonstrate the effect of variations in the number of BPRs per assembly, Fig. 16 shows differences in  $k_{inf}$  values ( $\Delta k$  values relative to the no-BPR condition) as a function of burnup for an initial fuel enrichment of 4.0 wt%  $^{235}U$  for one- and three-cycle exposures, respectively. The reactivity effect increases linearly with the number of BPRs present, as is more clearly shown in Fig. 17, which plots the  $\Delta k$  values at 45 GWd/tonne U as a function of the number of BPRs present.

*IV.A.1.c. Absorber ( $^{10}B$ ) Depletion.* The presence of the BPRs within the assembly guide tubes hardens the neutron spectrum due to removal of thermal neutrons by capture in  $^{10}B$ . In addition, the BPRs harden the neutron spectrum by displacement of moderator. Thus, the BPRs continue to harden the neutron spectrum even after the neutron absorber material has been essentially depleted. Figure 18 plots the  $^{10}B$  atom density as a function of burnup for the various initial fuel enrichment cases considered and demonstrates the increased rate of depletion with decreasing initial fuel enrichment. To maintain constant fission power, lower  $^{235}U$  enrichment requires higher fuel flux, which leads to greater capture in  $^{10}B$ . The differences in the rate of  $^{10}B$  depletion with variations in initial fuel enrichment are also evident by comparing the slope of the  $\Delta k$  values in Fig. 15.

##### IV.A.2. Pyrex Burnable Absorber Assembly BPRs

The primary difference between the Westinghouse WABA and BAA BPRs is that the central annular gap is

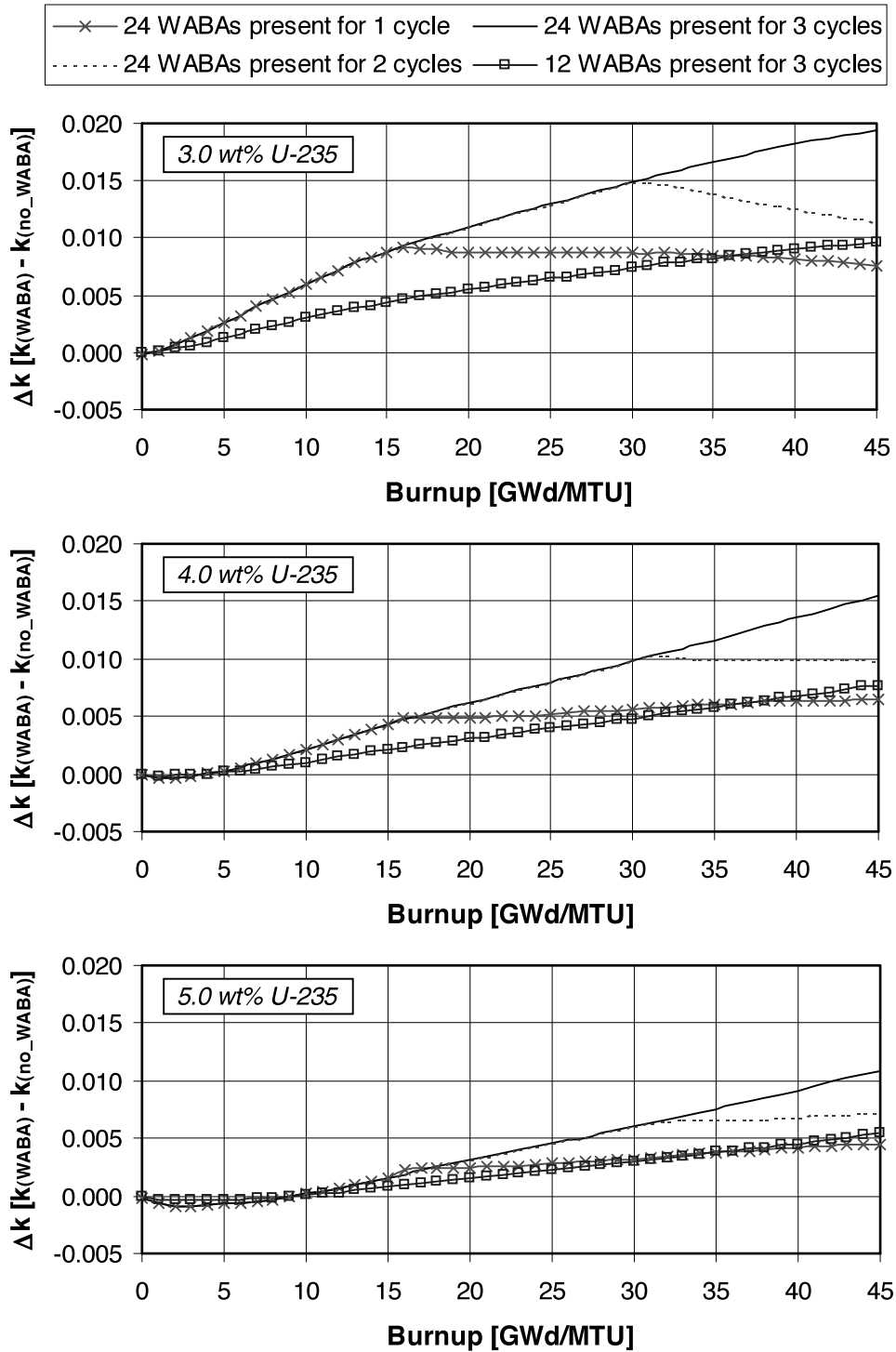


Fig. 15. The  $\Delta k$  values as a function of burnup for Westinghouse  $17 \times 17$  fuel with 3.0, 4.0, and 5.0 wt%  $^{235}\text{U}$  initial enrichment that has been exposed to Westinghouse WABA rods (three cycles of 15 GWd/tonne U per cycle were assumed).

dry in the BAA BPRs, while it is wet in the WABA BPRs. Thus, the BAA BPRs displace a greater volume of water and hence result in a larger effect on reactivity. An additional important difference is the cladding material;

BAAs use stainless steel, while WABAs use Zircaloy. Figure 19 shows the differences in  $k_{inf}$  values ( $\Delta k$  values relative to the no-BPR condition) associated with various exposures to BAA BPRs as a function of burnup for

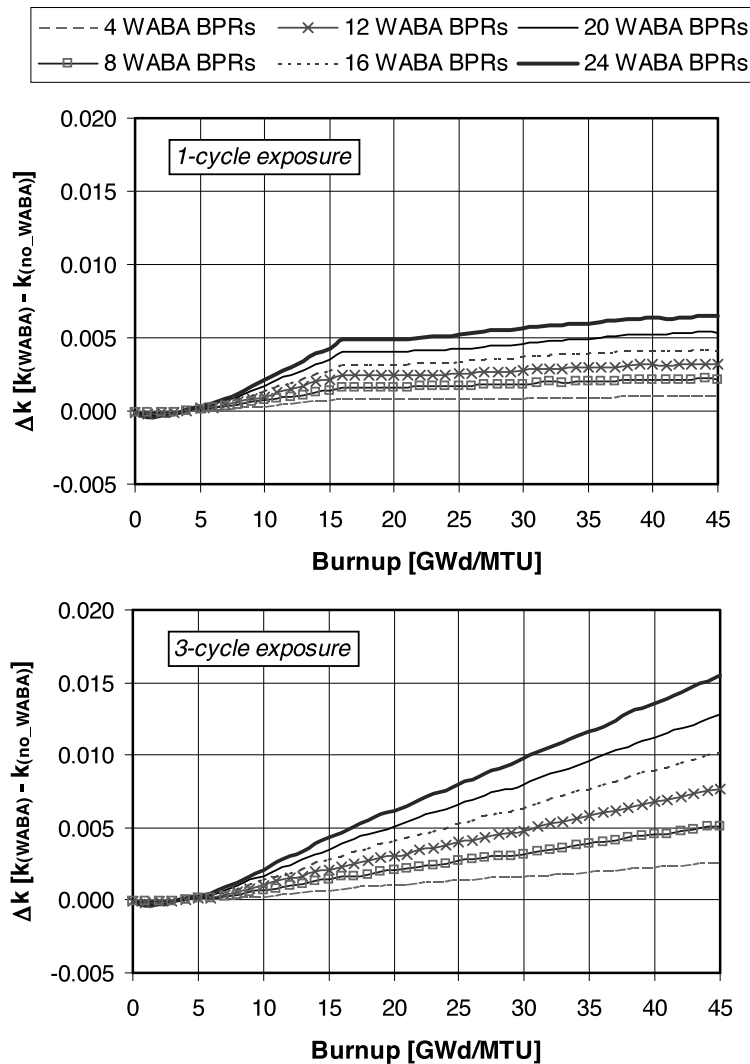


Fig. 16. The  $\Delta k$  values as a function of burnup for Westinghouse  $17 \times 17$  fuel with 4.0 wt%  $^{235}\text{U}$  initial enrichment that has been exposed to various numbers of Westinghouse WABA rods.

4.0 wt%  $^{235}\text{U}$  initial enrichment. The same trends identified with the WABA BPRs are also observed with the BAA BPRs; i.e., the reactivity effect increases with increasing BPR exposure and decreasing initial fuel enrichment. However, as expected, the BAA BPRs have a greater effect on reactivity. For initial enrichments of 3.0, 4.0, and 5.0 wt%  $^{235}\text{U}$ , maximum  $\Delta k$  values for continuous BAA BPR exposure up to a burnup of 45 GWd/tonne U are 0.0302, 0.0231, and 0.0159, respectively, as compared to 0.0194, 0.0155, and 0.0109, respectively, for the WABA BPRs.

#### IV.B. B&W BPR Designs

The B&W BPR design consists of solid rods containing  $\text{Al}_2\text{O}_3\text{-B}_4\text{C}$  clad in Zircaloy. Unlike the Westing-

house designs, the number of BPRs per assembly is generally fixed, and the weight percent of  $\text{B}_4\text{C}$  in the BPRs is varied.<sup>29-31</sup> Therefore, calculations were performed for a fixed number of BPRs present (i.e., 16 BPRs in a  $15 \times 15$  fuel assembly).

The primary differences between the B&W BPR design and the Westinghouse BPR designs are that the B&W BPRs are solid, have a fixed number of BPRs per BPRA, and may have varying poison ( $\text{B}_4\text{C}$ ) loading, as opposed to the Westinghouse designs which are annular, have varying numbers of BPRs per BPRA, and have fixed poison loadings. Actual plant data in Ref. 29 show variations in  $\text{B}_4\text{C}$  loading from 0.0 to 2.1 wt%. Since 2.0 wt%  $\text{B}_4\text{C}$  is approximately the maximum poison loading found in available plant data, initial calculations for the B&W BPRs used 2.0 wt%  $\text{B}_4\text{C}$ . Figure 20 shows the

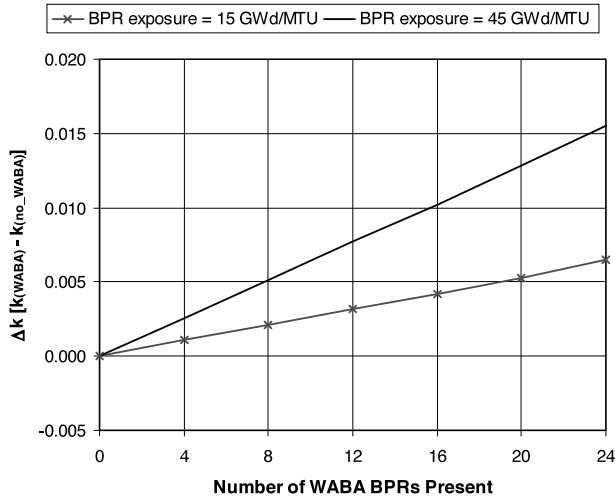


Fig. 17. The  $\Delta k$  values for Westinghouse  $17 \times 17$  fuel with 4.0 wt%  $^{235}\text{U}$  initial enrichment and a total burnup of 45 GWd/tonne U that has been exposed to various numbers of Westinghouse WABA rods for various burnup exposures.

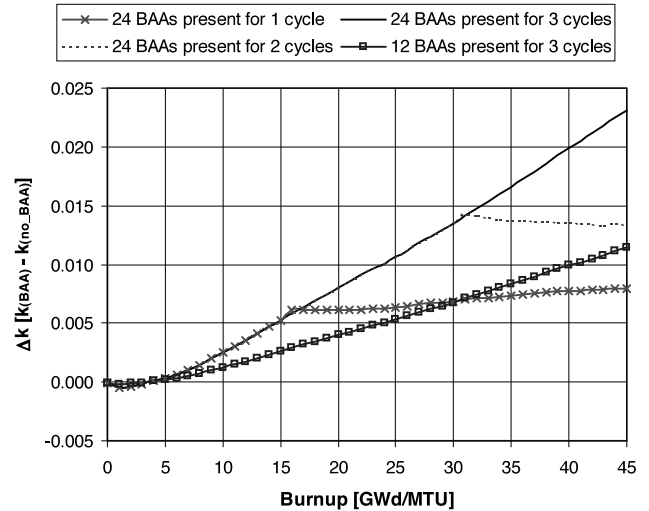


Fig. 19. The  $\Delta k$  values as a function of burnup for Westinghouse  $17 \times 17$  fuel with 4.0 wt%  $^{235}\text{U}$  initial enrichment that has been exposed to Westinghouse Pyrex BAA rods (three cycles of 15 GWd/tonne U per cycle were assumed).

differences in  $k_{inf}$  values ( $\Delta k$  values relative to the no-BPR condition) associated with various exposures to B&W BPRs as a function of burnup for 4.0 wt%  $^{235}\text{U}$  initial enrichment. The same trends identified with the

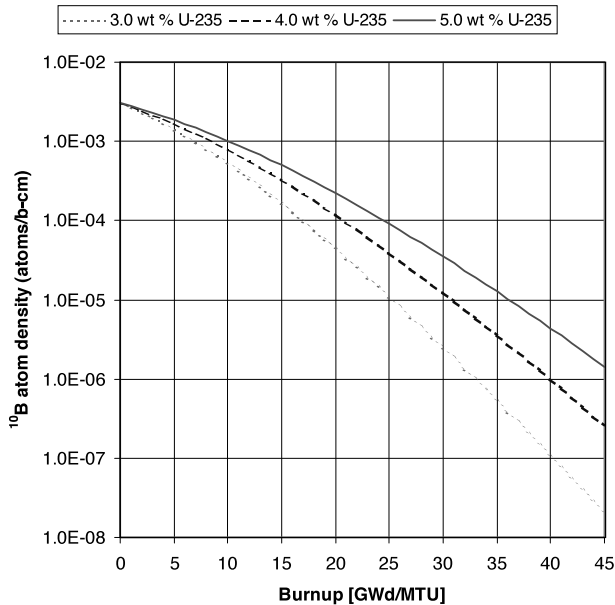


Fig. 18. The  $^{10}\text{B}$  atom density as a function of burnup for various cases of initial fuel enrichment. The results correspond to 24 Westinghouse WABA rods inserted into Westinghouse  $17 \times 17$  fuel with various initial enrichments during the entire depletion.

Westinghouse BPRs are also observed with the B&W BPRs; the reactivity effect increases with increasing BPR exposure and decreasing initial fuel enrichment. The B&W BPRs have an effect comparable to the Westinghouse WABA BPRs. For initial enrichments of 3.0, 4.0, and 5.0 wt%  $^{235}\text{U}$ ,  $\Delta k$  values for continuous B&W BPR exposure up to a burnup of 45 GWd/tonne U are 0.0204, 0.0155, and 0.0106, respectively. When considering these (and the previous) quoted maximum  $\Delta k$  values, the reader should be mindful that they are not representative of actual plant operations but are based on bounding calculational assumptions (e.g., BPR exposure during all three cycles of burnup, maximum number of BPRs per BPR in the case of Westinghouse BPRs, and nearly maximum poison loading in the case of the B&W BPRs).

#### IV.B.1. Effect of Variations in the BPR Poison ( $B_4C$ ) Loading

From plant data, the initial  $B_4C$  content in B&W BPRs is as high as 2.1 wt%. Calculations were performed for loadings from 0 to 3 wt% as an upper bound. Figure 21 shows the reactivity differences ( $\Delta k$  values relative to the no-BPR condition) as a function of burnup for an initial fuel enrichment of 4.0 wt%  $^{235}\text{U}$  and one-cycle exposure. The significance of the moderator displacement is apparent in the case with 0 wt%  $B_4C$ , in which case the BPR is composed of  $\text{Al}_2\text{O}_3$ . The reactivity effect increases linearly with the poison loading, as is more clearly shown in Fig. 22, which plots the  $\Delta k$  values at 45 GWd/tonne U as a function of poison loading.

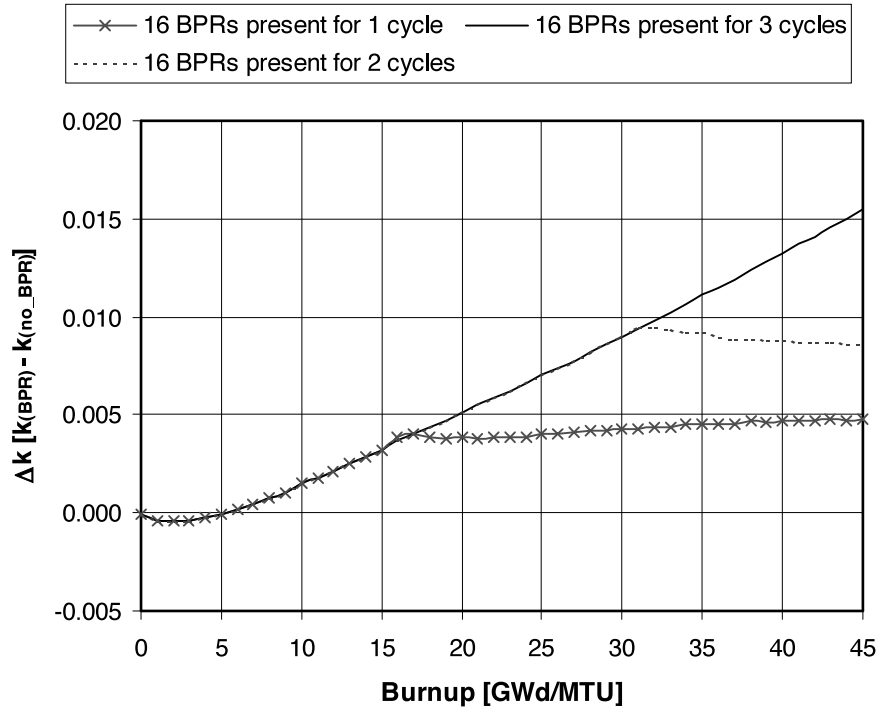


Fig. 20. The  $\Delta k$  values as a function of burnup for B&W  $15 \times 15$  fuel with 4.0 wt%  $^{235}\text{U}$  initial enrichment that has been exposed to B&W (2.0 wt%  $\text{B}_4\text{C}$ ) BPRs (three cycles of 15 GWd/tonne U per cycle were assumed).

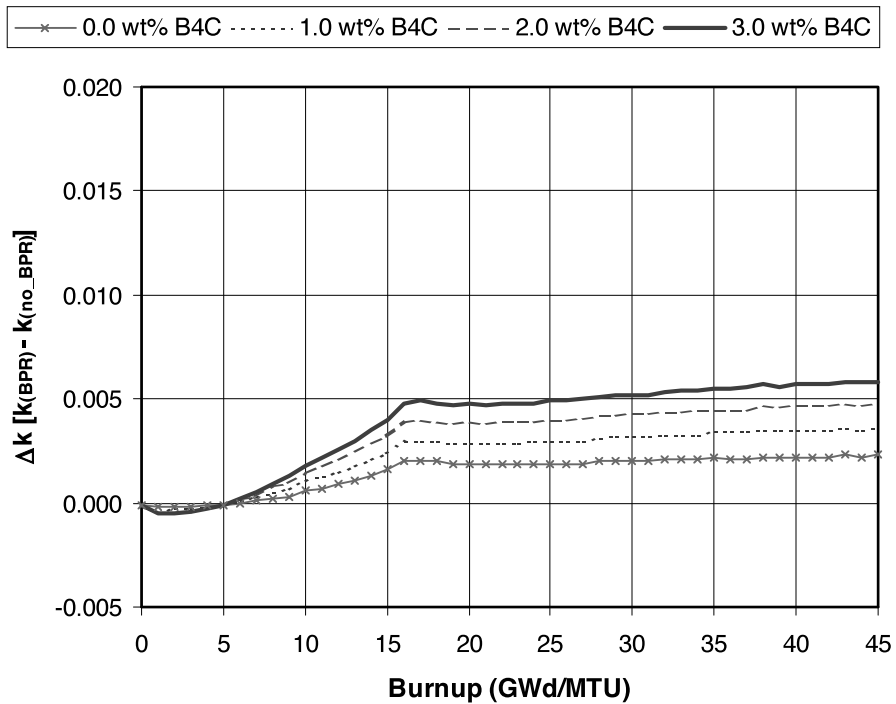


Fig. 21. The  $\Delta k$  values as a function of burnup for B&W  $15 \times 15$  fuel with 4.0 wt%  $^{235}\text{U}$  initial enrichment that has been exposed to B&W BPRs with varying  $\text{B}_4\text{C}$  weight percents for the first 15 GWd/tonne U of burnup (three cycles of 15 GWd/tonne U per cycle were assumed).

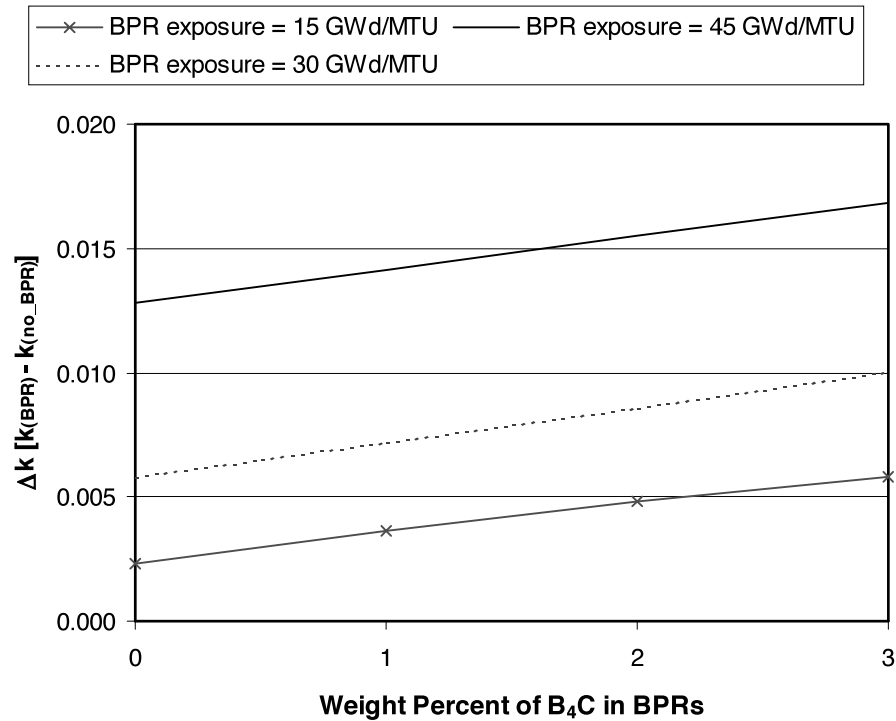


Fig. 22. The  $\Delta k$  values for B&W  $15 \times 15$  fuel with 4.0 wt%  $^{235}\text{U}$  initial enrichment and a total burnup of 45 GWd/tonne U that has been exposed to BPRs with varying poison loading and burnup exposures.

#### IV.C. Additional Studies and Discussion

As this study was performed in support of burnup credit, a number of the aforementioned calculations were repeated with modeling assumptions and conditions associated with typical burnup credit studies and analyses to assess their impact on the results. In particular, the effect of cask geometry (presence of fixed absorbers), cooling time, and axial burnup distribution were studied for selected cases. In addition, calculations were performed to assess the consequence to reactivity of loading assemblies with three-cycle BPR exposure into a cask intended to contain assemblies with one-cycle BPR exposure. Finally, code-to-code comparisons between HELIOS and the SAS2H (Ref. 32) depletion sequence from SCALE (Ref. 12) were performed to assess the ability of independent codes and methods and cross-section libraries to predict the reactivity effect of BPRs.

##### IV.C.1. Cask Calculations

The results in the previous sections provide understanding of the behavior of reactivity as a function of the relevant variables (e.g., burnup, enrichment, and BPR design) when assemblies are exposed to BPRs. In this section, the reactivity effect of BPRs within a realistic high-capacity rail-type cask (i.e., the GBC-32 cask) is examined and quantified. The 3-D cask criticality calcu-

lations were performed with KENO V.a using spent-fuel isotopics from HELIOS depletion calculations.

The  $k_{eff}$  values for actinide-only and actinide + fission product burnup-credit nuclides in the GBC-32 cask, assuming uniform axial burnup, for various BPR exposures are shown in Fig. 23. The results correspond to SNF with 4.0 wt%  $^{235}\text{U}$  initial enrichment and 45 GWd/tonne U burnup that has been exposed to each of the three BPR types considered previously. Unlike the results presented in previous sections, all results in this section correspond to 5-yr cooling time, which is more typical of burnup-credit analyses. The relative behavior is the same as that exhibited in the previous subsections for infinite arrays of assemblies at zero cooling time, and good agreement between the  $\Delta k$  values determined via 3-D cask calculations and those determined using infinite assembly array calculations is observed. In addition, comparison of the results for actinide-only and actinide + fission products (in Fig. 23) shows no significant differences.

##### IV.C.2. Effect of Axial Burnup Distribution

To demonstrate the impact of incorporating the axial burnup distribution, the  $k_{eff}$  values for actinide-only and actinide + fission product burnup credit in the GBC-32 cask, including the axial burnup distribution, for various BPR exposures were also calculated.<sup>7</sup> In comparison to

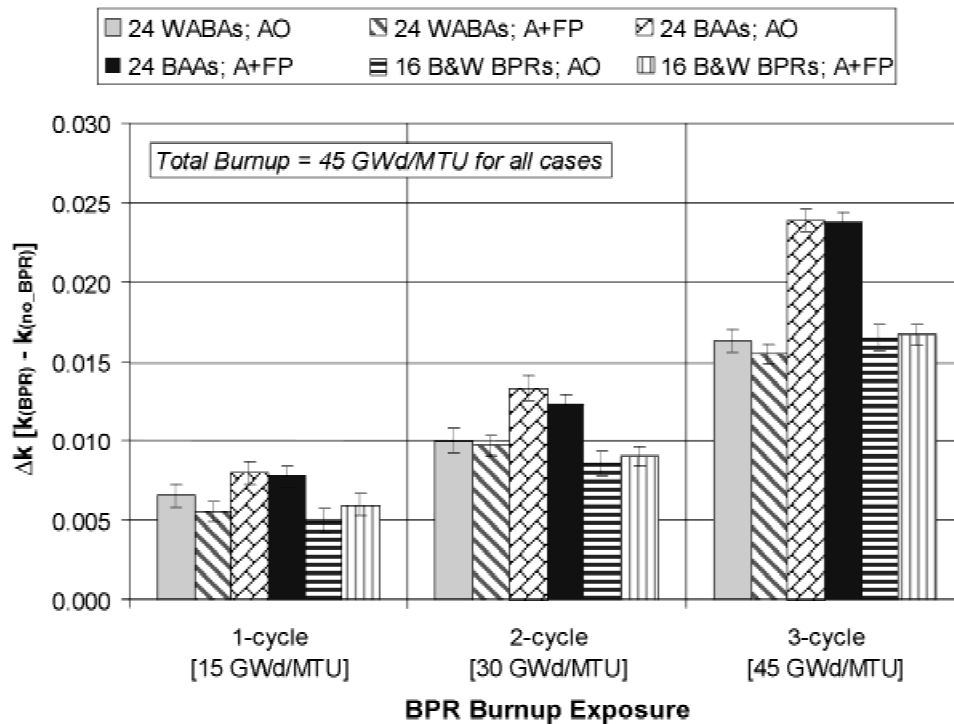


Fig. 23. Comparison of  $\Delta k$  values in the GBC-32 cask (45 GWd/tonne U, 5-yr cooling) for various BPR exposures as calculated with KENO V.a based on isotopics from HELIOS for actinide-only (AO) and actinide + fission product (A+FP) burnup credit. The results correspond to fuel with 4.0 wt%  $^{235}\text{U}$  initial enrichment that has been exposed to the various types of BPRs for one, two, and three cycles. Error bars correspond to  $1\sigma$  uncertainties in the  $\Delta k$  values.

results with uniform axial burnup, the inclusion of the axial burnup distribution was found to lessen the reactivity increase associated with the use of BPRs. This is due to the fact that with the axial burnup distribution included, the underburned end regions that dominate the reactivity of the fuel<sup>22</sup> achieve less burnup (than the assembly average) while the BPRs are inserted.

#### IV.C.3. Consideration of Risk-Based Approaches

Considering that BPRs are typically used during the first cycle only, assuming maximum (three-cycle) BPR exposure is not consistent with actual reactor operational practice. However, consideration of only one-cycle exposure in a safety evaluation would likely require justification of the one-cycle assumption or specific limitations on cask loading (i.e., exclusion of assemblies exposed to BPRs for more than one cycle).

Therefore, an analysis was performed with the GBC-32 cask to assess the impact of loading one or more assemblies that have BPR exposure that exceeds the one-cycle assumption. The analysis was performed for a burnup of 45 GWd/tonne U and 5-yr cooling. The more reactive assemblies were assumed to have three-cycle exposure to WABA BPRs, and the calculations assumed that the assemblies with the more reactive BPR exposure

(i.e., three cycles) were loaded from the center outward. The remaining assemblies were assumed to have one-cycle exposure to WABA BPRs. The results are shown in Fig. 24 for calculations for actinide-only burnup credit and confirm the relatively small reactivity consequence associated with loading a small number of assemblies with significantly greater BPR exposure (i.e., three cycles). Note that three-cycle BPR exposure exceeds any known operational practice. Results are shown in Fig. 24 for multiple loadings of assemblies with more reactive BPR exposure to demonstrate the associated impact on  $k_{eff}$ . The reactivity consequence of loading a single assembly with three-cycle exposure, as compared to the one-cycle exposure, is shown to be  $\sim 0.001 \Delta k$ . Further, approximately five three-cycle exposure assemblies are required (clustered together in the center of the cask) to raise the  $k_{eff}$  of the cask by  $0.005 \Delta k$ . Note that if the analysis had been performed assuming the more reactive assemblies had two-cycle BPR exposure, the reactivity effect would have been smaller.

The reactivity consequence of loading an assembly with greater BPR exposure will depend on the total burnup and the reference BPR exposure assumed for the remaining assemblies. If one considers the likelihood of the existence of assemblies with three-cycle BPR exposure

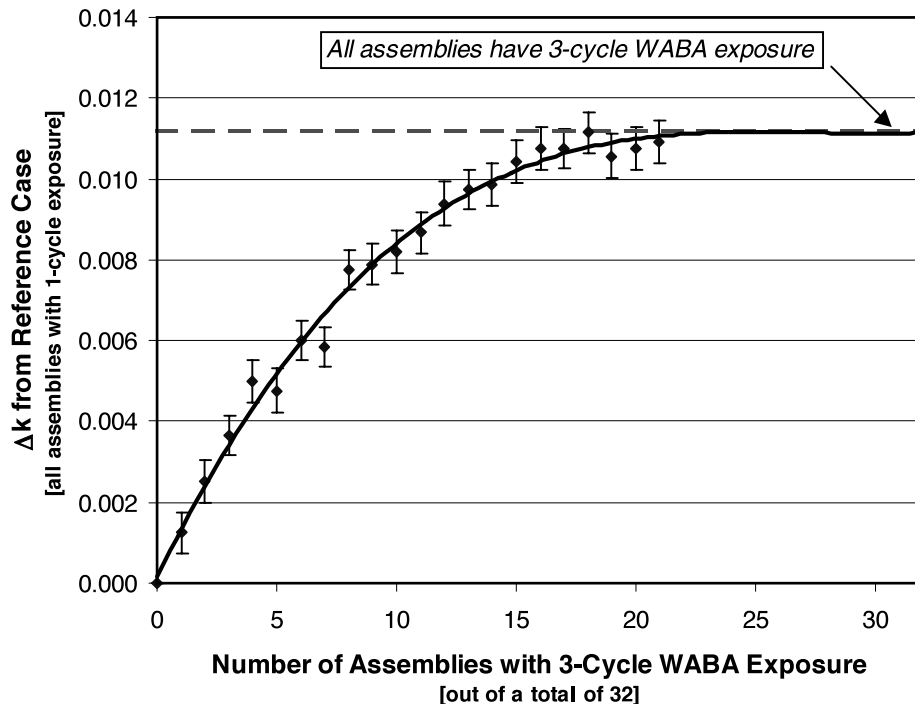


Fig. 24. Increase in  $k_{eff}$  due to loading assemblies with three-cycle BPR exposure into a GBC-32 cask in which the remaining assemblies have one-cycle BPR exposure. The results correspond to Westinghouse  $17 \times 17$  fuel with 4.0 wt%  $^{235}\text{U}$ , total burnup of 45 GWd/tonne U, Westinghouse WABA rods, actinide-only nuclides, and 5-yr cooling time.

and the relatively small impact on the cask  $k_{eff}$ , the use of an adequate one-cycle exposure might be justified in a safety evaluation. Note, however, that it is necessary to determine an appropriate assembly-average burnup for the one-cycle exposure assumption (e.g., 15 GWd/tonne U is likely too low to bound one-cycle exposure in actual discharged SNF).

#### IV.C.4. Comparison of SAS2H and HELIOS Results

The SCALE depletion sequence, SAS2H, has been extensively used (e.g., Refs. 10, 13, 20, 33, and 34) and validated (e.g., Refs. 35, 36, and 37) in studies of the burnup-credit phenomenon. Nevertheless, the HELIOS code was selected as the primary depletion tool for this analysis because of its capability to explicitly model the relatively complicated, heterogeneous assembly lattices associated with the fixed absorbers. Consequently, it is desirable to compare results from these two codes.

As validation of isotopic predictions for assemblies with fixed absorbers is hindered by a paucity of applicable measured isotopic data, HELIOS and SAS2H results were compared for a selected number of cases. Although a code-to-code comparison lacks the rigor of a direct comparison to measured SNF data, such a comparison does enable an assessment of the relative behavior of the two codes.

The presence of BPRs challenges the SAS2H modeling capabilities. A SAS2H fuel assembly model is limited to a one-dimensional radial model with a single smeared fuel region. Geometric modeling approximations are made in an effort to achieve a reasonable assembly-averaged neutron energy spectrum during the depletion process. For a select number of cases, isotopics were calculated with the SAS2H sequence, which uses ORIGEN-S for depletion. All SAS2H calculations utilized the SCALE 44-group (ENDF/B-V) library and were performed using the same depletion parameters used for the HELIOS calculations (see Sec. II). To enable a consistent comparison of the depletion isotopics on reactivity, isotopics were extracted from both HELIOS and SAS2H for use in consistent KENO V.a criticality models of the GBC-32 cask. The differences in the predicted  $k_{eff}$  values ( $\Delta k$  values) as a function of burnup based on isotopics calculated separately by SAS2H and HELIOS were compared for each of the aforementioned three types of BPRs and found to be within a few tenths of a percent, with SAS2H isotopics generally predicting slightly greater reactivity effects.<sup>7</sup> Despite the fact that the two codes use different cross sections (ENDF/B-V for SAS2H and ENDF/B-VI for HELIOS), good agreement was observed. Moreover, good agreement between calculated  $k_{eff}$  values based on isotopics from SAS2H and HELIOS was achieved.

#### IV.D. Summary of BPR Analyses

The results presented in this section demonstrate that the reactivity effect of BPRs increases with increasing burnup exposure and BPR poison loading (number of BPRs/BPRA and  $^{10}\text{B}$  wt%) and decreasing initial fuel enrichment. Although variations are observed for the different BPR designs, maximum reactivity increases were found to be within 1 to 3%  $\Delta k$ , when maximum BPR loading and exposure time are assumed. Expected typical reactivity increases, based on one-cycle exposure, were found to be  $<1\%$   $\Delta k$ . Of the BPR designs considered, the Westinghouse BAA BPR design yields the greatest positive reactivity effect. Although BPR poisons are effectively depleted during the first cycle of exposure, a significant portion of the reactivity difference is associated with the displacement of moderator.

The analyses provide a technical basis for burnup credit for assemblies that have used BPRs. Although the analyses do not address the issue of validation of depletion methods for assembly designs with BPRs, they do demonstrate that the effect of the BPRs is generally well behaved and that independent codes and cross-section libraries predict very similar results. Guidance should require safety analyses to include the effect of BPRs for assemblies that are classified as acceptable contents for the particular cask. For example, safety analyses for casks that are to be loaded with assemblies that contained BPRs during irradiation should account for the limiting BPR irradiation justified by the applicant's operations and design information and/or verified during cask loading. Assuming maximum BPR exposure during depletion would be a simple, conservative approach to bound the reactivity effect of BPRs. However, more realistic approaches based on typical operating conditions and/or loading restriction(s) may be acceptable with supporting justification (e.g., loading verification, analyses of statistically representative plant operating data, consideration of the impact on reactivity associated with loading assemblies that have greater than assumed BPR exposure, etc.).

While it is known that BPRs are typically inserted into an assembly during its first cycle of operation and subsequently withdrawn, exceptions to this practice do exist. If analyses were accompanied by administrative restrictions to ensure that assemblies with greater than one cycle of BPR exposure were not accepted for loading, analyses could be performed based on only a single cycle of BPR exposure. Such an approach would require the maximum-single cycle exposure to be defined such that all (or most) single-cycle BPR exposures are bounded. A complication associated with this approach is the necessity of plant data specifying assembly BPR exposure. Considering the large degree of conservatism (2 to 3%  $\Delta k$ ) associated with assuming the BPRs are present throughout the entire irradiation, the additional complexities of such administrative controls may be considered acceptable by burnup-credit applicants.

#### V. ANALYSES FOR CONTROL RODS

The presence of CRs/APSRs increases the reactivity of burned fuel by hardening the neutron spectrum (due to removal of thermal neutrons by capture and by displacement of moderator) and suppressing burnup in localized regions. The latter effect can lead to axial burnup distributions characterized by significantly underburned regions, as is apparent by examining several of the axial burnup distributions in the Yankee Atomic axial burnup profile database.<sup>16</sup> Although the axial burnup distribution is an important concern for burnup-credit evaluations, the effect of CR/APSR insertion on the axial burnup distribution is not addressed here because it is considered in the selection of bounding axial burnup profile(s).<sup>13,38</sup> Instead, this study examines the effect of CR/APSR insertion on reactivity due to the impact of spectral hardening on the spent-fuel isotopics.

Currently in the United States, PWRs operate with the CRs withdrawn or nearly withdrawn and use soluble boron to control the change in reactivity with burnup. In contrast, French PWR operations involve long periods of CR insertion for reactor control, low-power operations, and load-following.<sup>39</sup> Similarly, some early domestic operations included notable CR insertions (usually in conjunction with an assembly's first cycle of burnup).<sup>29</sup> Axial power shaping rods are inserted during normal operation but are less common [e.g., in Three Mile Island unit 1, eight assemblies/core may contain APSRs, while 24 assemblies/core may contain CRs (Ref. 40)]. Fuel shuffling between cycles reduces the probability that a fuel assembly will be exposed to CR/APSR insertions for more than one cycle.

Due to the potentially great variability in CR and APSR usage, estimating the effect of CRs and APSRs in a generic manner is difficult. Based on operational arguments for U.S. PWRs, similar to those stated previously, an earlier study<sup>13</sup> considered full-axial insertion for one cycle (15 GWd/tonne U) as an upper bound for assemblies exposed to CRs. For this evaluation, similar to the approach in the previous section for BPRs, parametric analyses were performed for a variety of exposure scenarios, including partial insertion, to establish an increased understanding of the effect of CR exposure on the reactivity of discharged SNF. Although many of the scenarios considered are not representative of current U.S. PWR operations, it is possible to estimate the reactivity effect of specific CR exposure conditions based on inspection of the calculated results and trends developed in this evaluation. Further, the scenarios may have relevance to early domestic and non-U.S. PWR operations.

The evaluation was performed in two parts. In the first part, calculations were performed assuming full-axial CR exposure (i.e., fully inserted). These calculations were intended to bound the effect of CR exposure and facilitate comparisons of the various CR designs. In the second part, calculations were performed to

determine the effect of various axial insertion depths and gain a better understanding for current U.S. PWR operations. Note that the effect of the CRs was determined based on their effect on the depletion isotopics alone (i.e., the CRs are present for various intervals in the depletion calculations but are not present in the criticality models and calculations).

Numerous CR designs have been used in U.S. commercial nuclear reactors. However, all CR designs are similar in that they contain thermal neutron absorbing material in rods sized to fit within assembly guide tubes. Although the variation in CR designs is significant, the variation in CR absorber materials is more limited, namely, B<sub>4</sub>C, Ag-In-Cd, Hf, INCONEL,<sup>b</sup> and stainless steel. Rather than attempt to investigate each of the numerous CR designs, which in many cases involve relatively minor differences, this study focused on investigating unique CR designs and materials to establish greater understanding. The effects of CR designs that use the same absorber material are expected to yield similar reactivity effects. The designs considered include (a) B&W Ag-In-Cd CRs, (b) Westinghouse hybrid Ag-In-Cd/B<sub>4</sub>C CRs, (c) CE B<sub>4</sub>C CRs, and (d) B&W gray APSRs. Note that B&W (now Framatome ANP) is the only U.S. PWR fuel vendor known to use APSRs.

#### V.A. B&W Silver-Indium-Cadmium Control Rods

The Ag-In-Cd rod cluster control assembly (RCCA) developed by B&W consists of 16 CRs. For each of the 3.0, 4.0, and 5.0 wt% <sup>235</sup>U initial enrichments, calculations were performed with a B&W 15 × 15 assembly for cases in which the CRs were withdrawn at 5, 15, 30, and 45 GWd/tonne U (full exposure). The results ( $\Delta k$  as a function of burnup) are shown in Fig. 25. As expected, the reactivity effect of the CRs increases with increasing burnup exposure and decreasing fuel enrichment. The trends are consistent with those shown for BPRs in the previous section. However, the magnitude of the  $\Delta k$  values is notably higher for the CRs. The maximum positive  $\Delta k$  values for each of the cases considered are summarized in Table V, where the highest  $\Delta k$  value is shown to be ~7%.

The reactivity effect of CR exposure was also studied for scenarios in which the CRs were inserted for burnup periods of 5 GWd/tonne U throughout the assembly burnup. The results ( $\Delta k$  as a function of burnup) are shown in Fig. 26 for an initial enrichment of 4.0 wt% <sup>235</sup>U and demonstrate that CR exposure has a larger effect on discharge reactivity when it occurs later in the assembly burnup. Note that these calculations were performed to investigate and demonstrate the behavior and do not necessarily represent realistic conditions. However, some early U.S. PWR operations included significant CR insertions in conjunction with an assembly's

<sup>b</sup>INCONEL is a trademark of the Inco family of companies.

TABLE V

Maximum Positive  $\Delta k$  Values Observed for CR/APSR Cases Considered\*

| Burnup at Which CRs Are Removed (GWd/tonne U)   | Enrichment (wt% <sup>235</sup> U) |        |        |
|---|-----------------------------------|--------|--------|
|   | 3.0                               | 4.0    | 5.0    |
| B&W Ag-In-Cd CR Cases   |                                   |        |        |
| 5   | 0.0042                            | 0.0026 | 0.0017 |
| 15  | 0.0177                            | 0.0099 | 0.0063 |
| 30  | 0.0443                            | 0.0266 | 0.0154 |
| 45 <sup>a</sup>   | 0.0697                            | 0.0480 | 0.0304 |
| Westinghouse Hybrid Ag-In-Cd/B <sub>4</sub> C CR Cases (B <sub>4</sub> C Axial Segment) |                                   |        |        |
| 5   | 0.0086                            | 0.0048 | 0.0041 |
| 15  | 0.0280                            | 0.0174 | 0.0113 |
| 30  | 0.0698                            | 0.0417 | 0.0256 |
| 45 <sup>a</sup>   | 0.1050                            | 0.0739 | 0.0479 |
| CE Ag-In-Cd/B <sub>4</sub> C CR Cases (B <sub>4</sub> C Axial Segment)                  |                                   |        |        |
| 5   | 0.0045                            | 0.0028 | 0.0018 |
| 15  | 0.0213                            | 0.0121 | 0.0082 |
| 30  | 0.0553                            | 0.0339 | 0.0203 |
| 45 <sup>a</sup>   | 0.0866                            | 0.0619 | 0.0411 |
| B&W Gray (INCONEL) APSR Cases   |                                   |        |        |
| 5   | 0.0008                            | 0.0004 | 0.0002 |
| 15  | 0.0059                            | 0.0026 | 0.0017 |
| 30  | 0.0164                            | 0.0098 | 0.0057 |
| 45 <sup>a</sup>   | 0.0268                            | 0.0187 | 0.0121 |

\*Total burnup of 45 GWd/tonne U.

<sup>a</sup>Control rods present for entire depletion.

first burnup cycle.<sup>29</sup> Thus, it is expected that cases involving exposure during the first cycle (i.e., within the first 15 GWd/tonne U) are closer to reality than those involving exposure late in burnup.

#### V.B. Westinghouse Hybrid Ag-In-Cd/B<sub>4</sub>C Control Rods

The hybrid Ag-In-Cd/B<sub>4</sub>C RCCA developed by Westinghouse consists of 24 hybrid Ag-In-Cd/B<sub>4</sub>C CRs, each containing Ag-In-Cd absorber with B<sub>4</sub>C absorber pellets stacked on top. Since it is not possible to include axial variation in absorber material in a 2-D radial model and the effect of Ag-In-Cd CRs was demonstrated in the previous subsection for B&W fuel, a calculational model was developed to represent the axial segment corresponding to the B<sub>4</sub>C region. For each of the 3.0, 4.0, and 5.0 wt% <sup>235</sup>U initial enrichments, calculations were performed for cases in which the CRs were withdrawn at 5,

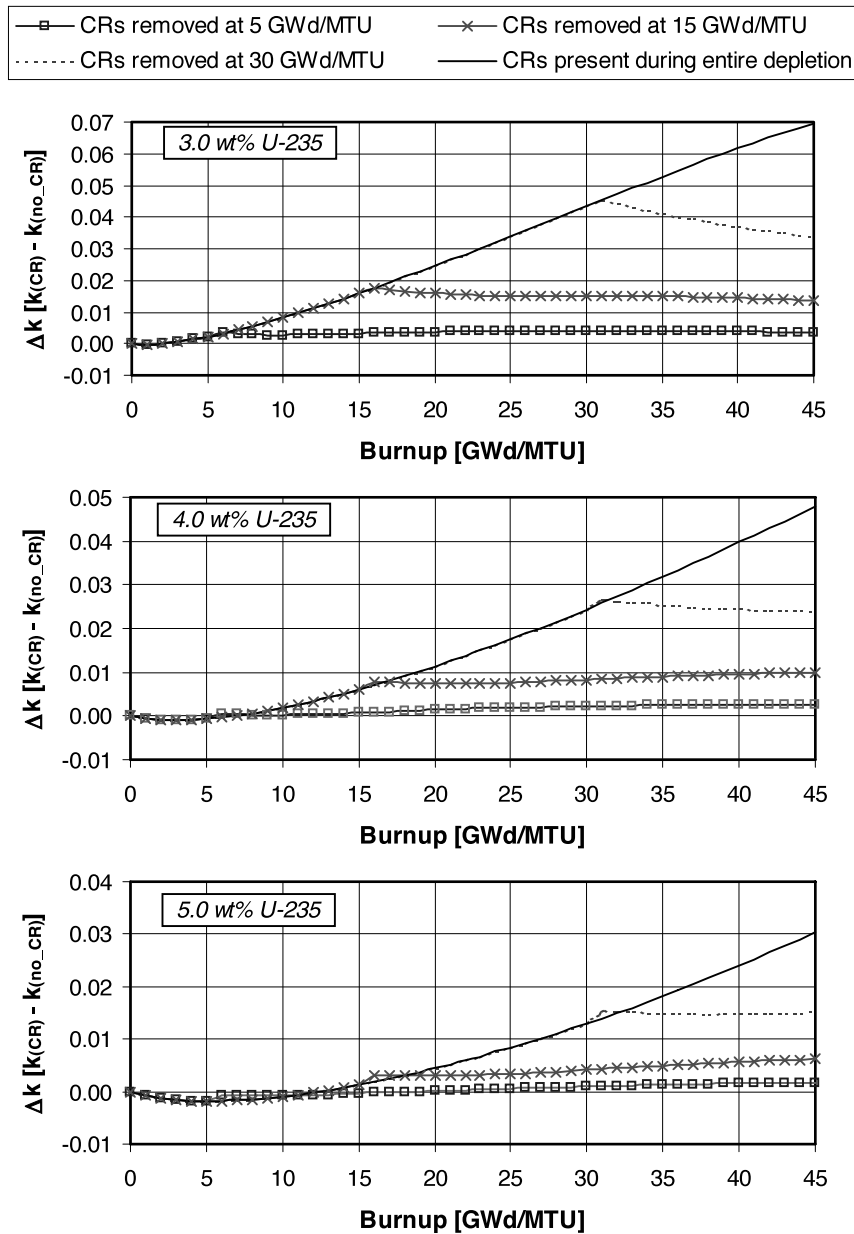


Fig. 25. The  $\Delta k$  values as a function of burnup for B&W  $15 \times 15$  fuel with 3.0, 4.0, and 5.0 wt%  $^{235}\text{U}$  initial enrichment that has been exposed to Ag-In-Cd CRs.

15, 30, and 45 GWd/tonne U (full exposure). The results ( $\Delta k$  as a function of burnup) are shown in Fig. 27 for the cases with 4.0 wt%  $^{235}\text{U}$  initial enrichment. Consistent with the results shown in the previous section, the reactivity effect of the CRs increases with increasing exposure and decreasing fuel enrichment. Note, however, the larger reactivity effect of the  $\text{B}_4\text{C}$  absorber, as compared to the Ag-In-Cd absorber considered in the previous section. The maximum positive  $\Delta k$  values for the cases considered are summarized in Table V, where the highest  $\Delta k$  value is  $\sim 10\%$ .

### V.C. CE Ag-In-Cd/ $\text{B}_4\text{C}$ Control Rods

CE has manufactured a variety of CR assemblies, referred to as control element assemblies (CEAs), for use in the 5 CR locations in their  $14 \times 14$  and  $16 \times 16$  fuel assembly designs.<sup>19</sup> Notable variations in absorber material type (e.g., stainless steel, INCONEL, Ag-In-Cd, and  $\text{B}_4\text{C}$ ), axial configuration, and length have been identified.<sup>31</sup> The CEA design considered in this study consisted of five INCONEL tubes (fingers) loaded with a stack of  $\text{B}_4\text{C}$  cylindrical pellets with the lower part of the

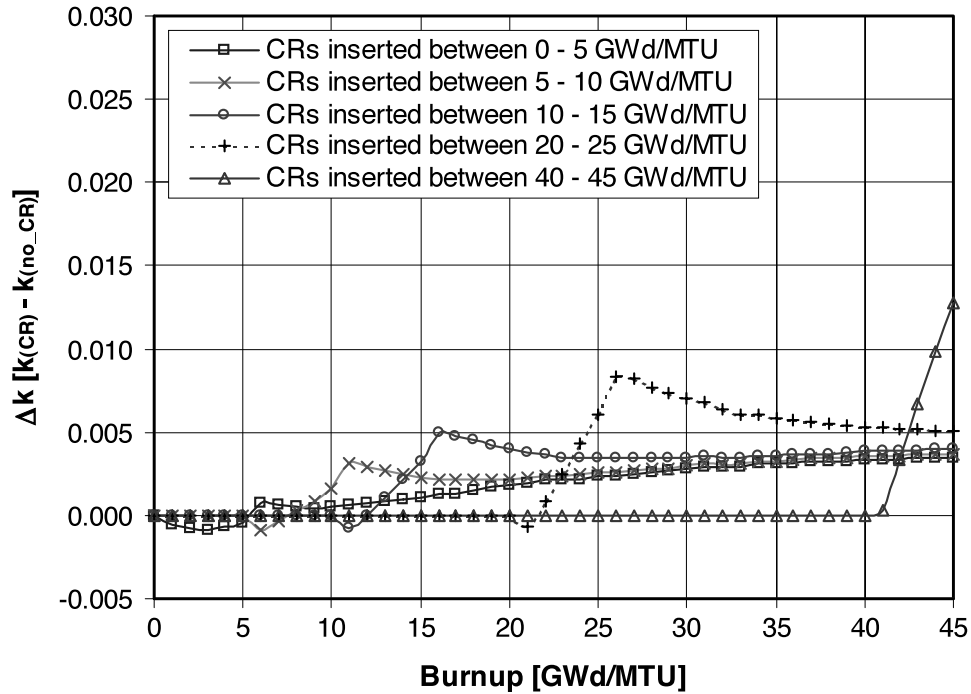


Fig. 26. The  $\Delta k$  values as a function of burnup for 5 GWd/tonne U CR exposures at various points during the burnup. Results correspond to B&W  $15 \times 15$  fuel with 4.0 wt%  $^{235}\text{U}$  initial enrichment and Ag-In-Cd CRs.

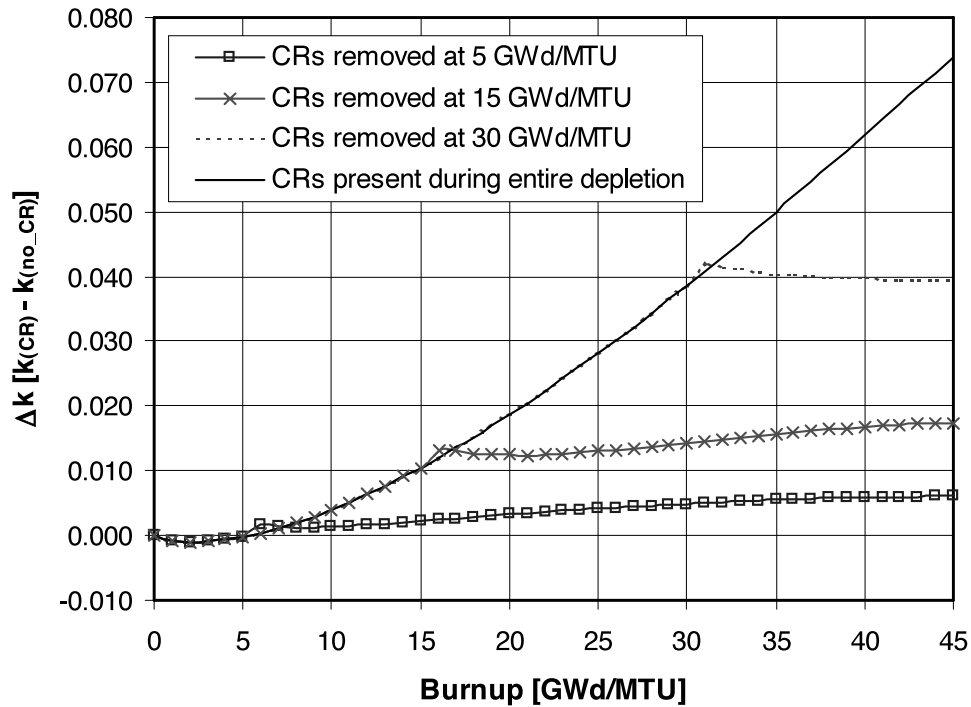


Fig. 27. The  $\Delta k$  values as a function of burnup for Westinghouse  $17 \times 17$  fuel with 4.0 wt%  $^{235}\text{U}$  initial enrichment that has been exposed to the  $\text{B}_4\text{C}$  axial segment of the hybrid Ag-In-Cd/ $\text{B}_4\text{C}$  CRs.

fingers containing Ag-In-Cd, for use with their 14 × 14 fuel assembly design. Analyses for this CR design, based on the B<sub>4</sub>C axial region and the initial enrichment and CR exposure conditions considered in the previous subsections, yielded results very similar to those shown in the previous subsection for Westinghouse CRs. However, the reactivity effect of the CE CRs was slightly less. The maximum positive Δk values are summarized in Table V, which shows that the highest Δk value is ~9%.

**V.D. B&W Gray Axial Power Shaping Rods**

In addition to the Ag-In-Cd CRs analyzed in Sec. V.A, B&W has developed gray part-length APSRs composed of INCONEL with stainless steel cladding. For each of the 3.0, 4.0, and 5.0 wt% <sup>235</sup>U initial enrichments, calculations were performed using a B&W 15 × 15 assembly for cases in which the APSRs were withdrawn at 5, 15, 30, and 45 GWd/tonne U (full exposure). The results (Δk as a function of burnup) are shown in Fig. 28 for 4.0 wt% <sup>235</sup>U initial enrichment. The maximum positive Δk values for the various APSR cases considered are summarized in Table V. Because the APSRs do not contain any strong thermal neutron absorbing materials, they have a significantly smaller reactivity effect compared to the CR designs. The highest observed Δk value was <3% Δk.

Based on a limited survey of operational data, it is difficult to characterize typical APSR operational practices. However, it is often the case that they are present during the majority of an assembly’s second burnup cycle, being withdrawn gradually late in the cycle. Therefore, calculations were performed for scenarios in which the APSRs were inserted during the first, second, and third cycles of burnup to quantify the reactivity effect. The results (Δk as a function of burnup) are shown in Fig. 29 for an initial enrichment of 4.0 wt% <sup>235</sup>U and demonstrate that consistent with the results shown previously for CRs, the APSR exposure has a larger effect on discharge reactivity when it occurs later in the assembly burnup. Note that the calculations were performed to investigate and demonstrate the behavior and do not necessarily represent realistic conditions. However, one can conclude that for realistic scenarios, such as APSR insertion during the entire second cycle, the effect is <1% Δk. Finally, note that because B&W is the only fuel vendor to use APSRs and <10 assemblies/core are exposed to APSRs, very few SNF assemblies are actually affected by APSRs

**V.E. Cask Calculations**

In current U.S. PWR operations, CRs are not ever fully inserted during power operations. The goal of the full-insertion analysis in the previous subsection was to

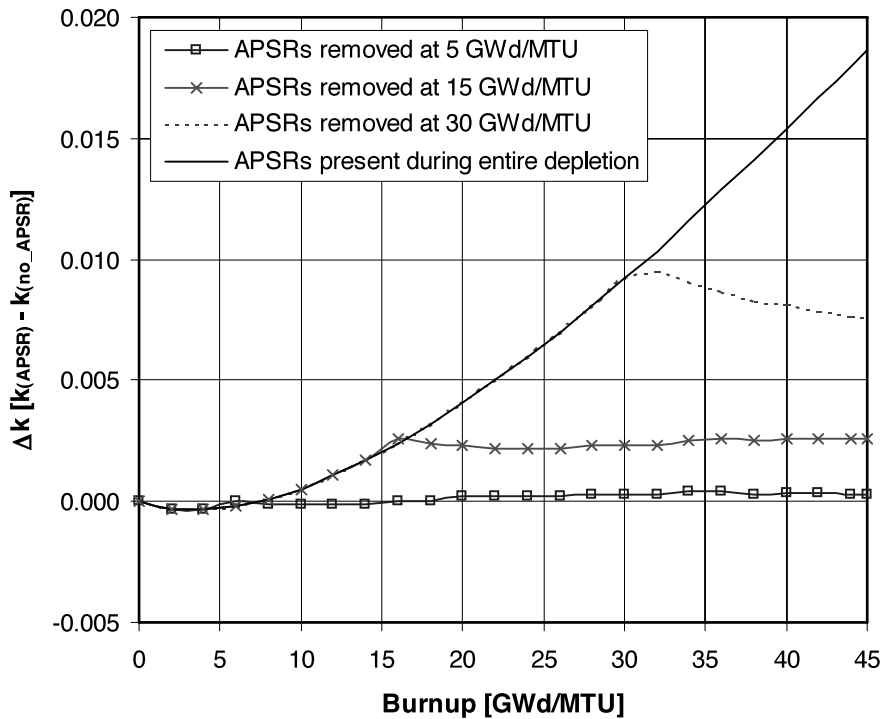


Fig. 28. The Δk values as a function of burnup for B&W 15 × 15 fuel with 4.0 wt% <sup>235</sup>U initial enrichment that has been exposed to gray (INCONEL) APSRs.

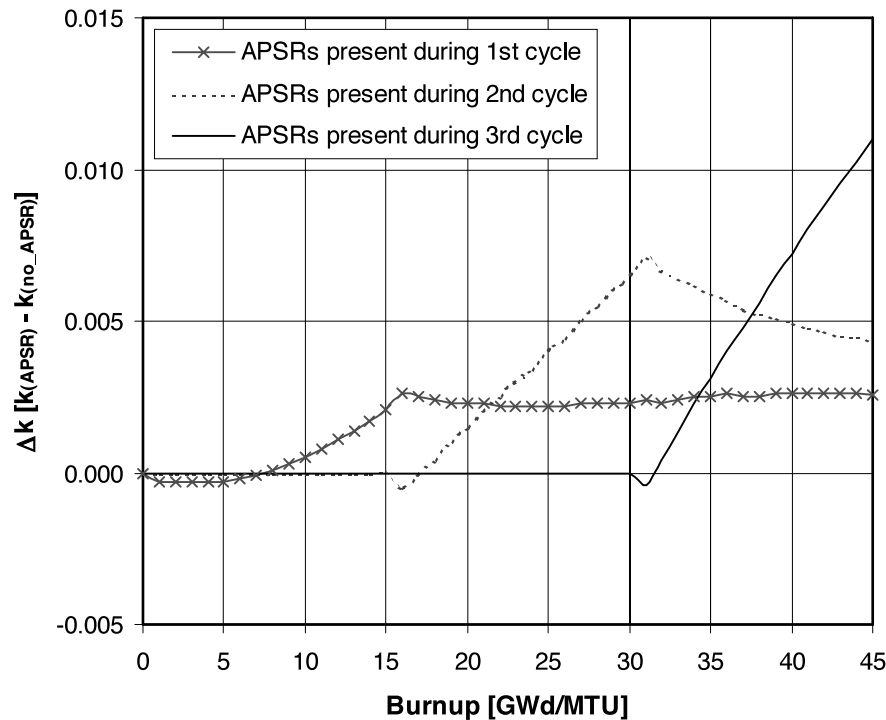


Fig. 29. The  $\Delta k$  values as a function of burnup for single-cycle APSR exposures. Results correspond to B&W  $15 \times 15$  fuel with 4.0 wt%  $^{235}\text{U}$  initial enrichment that has been exposed to gray (INCONEL) APSRs.

establish better understanding, trends, and upper bounds, and thus many of the scenarios overestimate the reactivity effect of CR exposure on actual discharged SNF. For current U.S. PWR operations, CRs are inserted into a small upper (top) portion of the active fuel; the remainder and majority of the time the CRs are inserted into the fuel assembly but are above the active fuel region. Realistic modeling of CR exposure should represent the partial axial insertion, which requires 3-D calculations. Therefore, 3-D cask calculations were performed and are presented in this section to establish a more realistic assessment of the effect of CR exposure on the reactivity of SNF.

Before explicitly considering variations in axial CR insertion depth, 3-D KENO V.a criticality calculations were performed with the GBC-32 cask for each of the aforementioned CR designs, assuming full-axial insertion. The KENO calculations included uniform axial isotopic compositions that were calculated with HELIOS. Comparison of the results to those shown previously for infinite assembly arrays showed that the CR effect is marginally greater in the cask configuration.<sup>8</sup> In addition, the  $\Delta k$  values based on actinide-only and actinide + fission product calculations in the GBC-32 cask were demonstrated to be essentially the same (i.e., the effect was not found to be very sensitive to the presence of fission products).

Subsequently, a series of 3-D KENO V.a calculations was performed for each CR design considered to determine the effect of various axial depths of CR insertion. The criticality models included isotopics from depletion calculations with CRs present (in the axial region representing CR insertion) and isotopics from depletion calculations without CRs present (in the remaining axial region).

The first series of calculations was performed with the Westinghouse  $17 \times 17$  assembly and the Westinghouse hybrid ( $\text{B}_4\text{C}/\text{Ag-In-Cd}$ ) CRs. Figure 30 shows the  $\Delta k$  values for actinide-only and actinide + fission product burnup credit in the GBC-32 cask as a function of axial depth of CR insertion. In accordance with the actual design, the axial variation in CR absorber material,  $\text{B}_4\text{C}$  in the top portion of the CR ( $\sim 260$  cm) and Ag-In-Cd in the bottom portion ( $\sim 102$  cm), was modeled. The results correspond to fuel with 4.0 wt%  $^{235}\text{U}$  initial enrichment that has been exposed to Westinghouse hybrid  $\text{B}_4\text{C}/\text{Ag-In-Cd}$  rods for 5, 15, and 45 GWd/tonne U, respectively, while accumulating a burnup of 45 GWd/tonne U. The KENO V.a models include the axial variation in the depletion isotopics due to CR exposure but assume uniform axial burnup. The results show that even for significant burnup exposures, shallow CR insertions (e.g.,  $< 20$  cm) result in an insignificant effect on the  $k_{\text{eff}}$  of a cask. Note also that for the cases with CRs, all

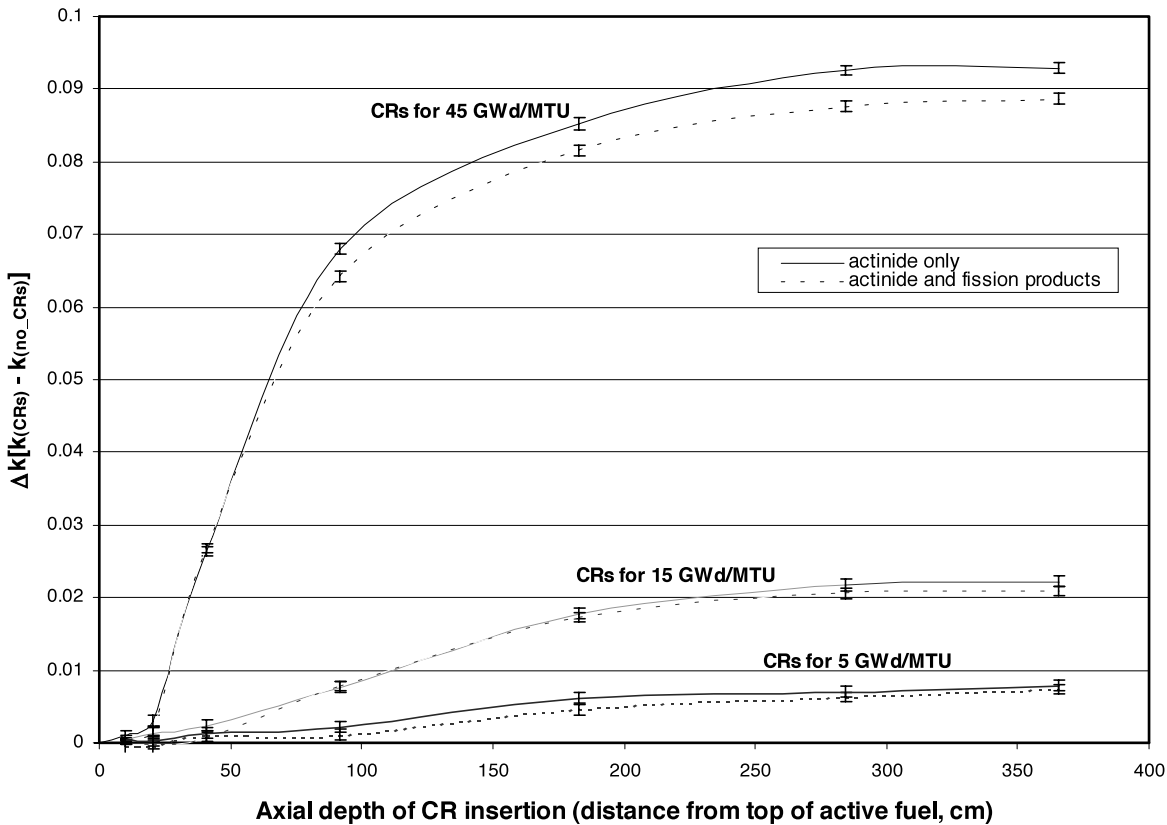


Fig. 30. The  $\Delta k$  values in the GBC-32 cask (45 GWd/tonne U, zero cooling) versus axial CR insertion, as calculated with KENO V.a based on isotopics from HELIOS for actinide-only and actinide + fission product burnup credit. The results correspond to Westinghouse  $17 \times 17$  fuel with 4.0 wt%  $^{235}\text{U}$  initial enrichment and hybrid Ag-In-Cd/ $\text{B}_4\text{C}$  CRs. Error bars correspond to  $1\sigma$  uncertainties in the  $\Delta k$  values.

assemblies in the 32-assembly GBC-32 cask are assumed to have the same CR exposure, which is conservative considering the number of assemblies per core that are positioned under RCCAs.

The calculations were repeated for the B&W  $15 \times 15$  fuel assemblies employing Ag-In-Cd CRs and the CE  $14 \times 14$  fuel assemblies employing Ag-In-Cd/ $\text{B}_4\text{C}$  CRs. The  $\Delta k$  values for actinide-only and actinide + fission product burnup credit in the GBC-32 cask with the various axial CR exposures are shown in Figs. 31 and 32, respectively. Consistent with the results for the Westinghouse hybrid CRs, the effect of minor axial CR insertions is shown to be insignificant. Further, the effect is shown to be notably smaller for both the B&W Ag-In-Cd and CE Ag-In-Cd/ $\text{B}_4\text{C}$  CRs than that shown for the Westinghouse hybrid Ag-In-Cd/ $\text{B}_4\text{C}$  CRs.

#### V.F. Summary of Control Rod Analyses

Due to spectral hardening, an assembly exposed to CRs will have a higher reactivity for a given burnup than an assembly that has not been exposed to CRs. For the various CR designs considered, maximum reactivity

increases were shown to be between 3 and 10%  $\Delta k$ , depending on initial enrichment, when maximum worst-case (full axial insertion for entire depletion) CR exposure was assumed for a total burnup of 45 GWd/tonne U. The reactivity effect of APSRs was shown to be significantly less than that of the CRs (for a given burnup exposure), with maximum reactivity increases between 1 and 3%  $\Delta k$ . The calculations assuming full-axial CR insertion for long periods of burnup simulated worst-case conditions but were effective for gaining a better understanding of the impact of CR exposure and establishing an upper bound on the reactivity effect. Although these cases are not considered to be representative of current U.S. PWR operations, they may have relevance to early domestic operations and operating conditions in French PWRs, which involve long periods of CR insertion for reactor control, low-power operations, and load-following.<sup>39</sup> Proposed approaches for burnup credit in France include full CR insertion.

The second part of the analysis presented the effect of CRs within a high-capacity rail-type cask designed for burnup credit. For each CR design considered, a series of 3-D KENO V.a calculations were performed to

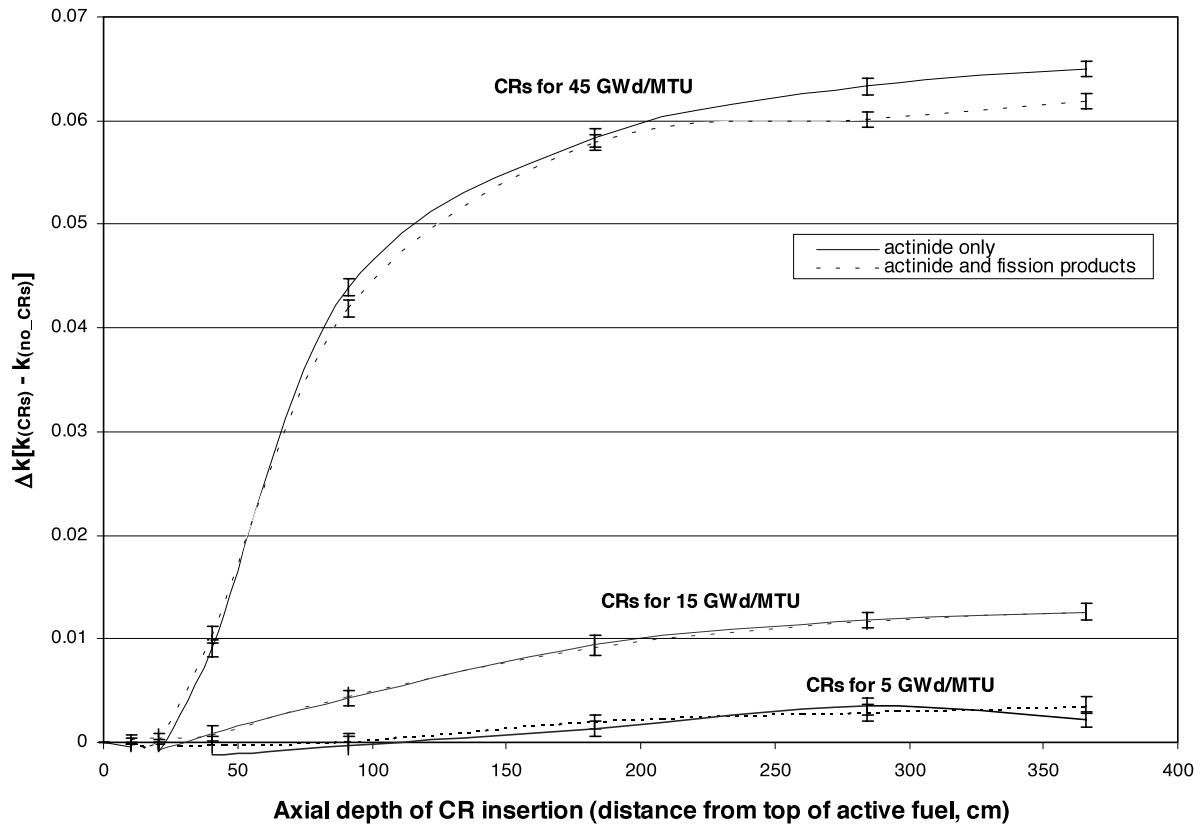


Fig. 31. The  $\Delta k$  values in the GBC-32 cask (45 GWd/tonne U, zero cooling) versus axial CR insertion, as calculated with KENO V.a based on isotopics from HELIOS for actinide-only and actinide + fission product burnup credit. The results correspond to B&W  $15 \times 15$  fuel with 4.0 wt%  $^{235}\text{U}$  initial enrichment and Ag-In-Cd CRs. Error bars correspond to  $1\sigma$  uncertainties in the  $\Delta k$  values.

determine the effect of various axial depths of CR insertion and thus achieve a better understanding of reality for current U.S. PWR operations. The results show that even for significant burnup exposures, minor axial CR insertions (e.g., <20 cm) result in an insignificant effect on the  $k_{eff}$  of the cask. Consequently, based on the assumption that current U.S. PWRs do not use CRs to a significant extent (i.e., CRs are not inserted deeper than the top  $\sim 20$  cm of the active fuel, and CRs are not inserted for extended burnups), it can be concluded that the effect of CRs on discharge reactivity is small ( $<0.2\%$   $\Delta k$ ). Note that the effect of CR/APSR insertion on the axial burnup distribution was not addressed here because it is considered in the selection of bounding axial profile(s).

## VI. SUMMARY AND CONCLUSIONS

The analyses described in this paper provide a technical basis to support burnup credit for assembly designs that have used fixed absorbers, including IBAs, BPRs, CRs, and APSRs. Trends in reactivity with rele-

vant parameters, such as initial fuel enrichment, burnup, and absorber exposure and design, for IBAs, BPRs, and CRs/APSRs are summarized in Secs. III, IV, and V, respectively. These studies demonstrate that with the exception of the Westinghouse IFBA rods, the IBA types considered here may be conservatively neglected from burnup-credit analyses. In contrast, BPRs were shown to have a notable positive impact on the reactivity of SNF for typical operating practices and thus must be properly addressed in a burnup-credit criticality safety evaluation. Finally, CRs and APSRs were shown to have notable positive effects that are strongly dependent on their usage. As an assembly cannot simultaneously accommodate BPRs and CRs and APSRs, the information within this paper could be used to support the position that the effect of BPRs bounds the effects of CRs and APSRs.

Although the analyses do not address validation of depletion methods for assembly designs with fixed absorbers, they do demonstrate that the effects are relatively small and generally well behaved. For the fixed absorber type that has the greatest effect on the reactivity of SNF, namely BPRs, independent codes and methods

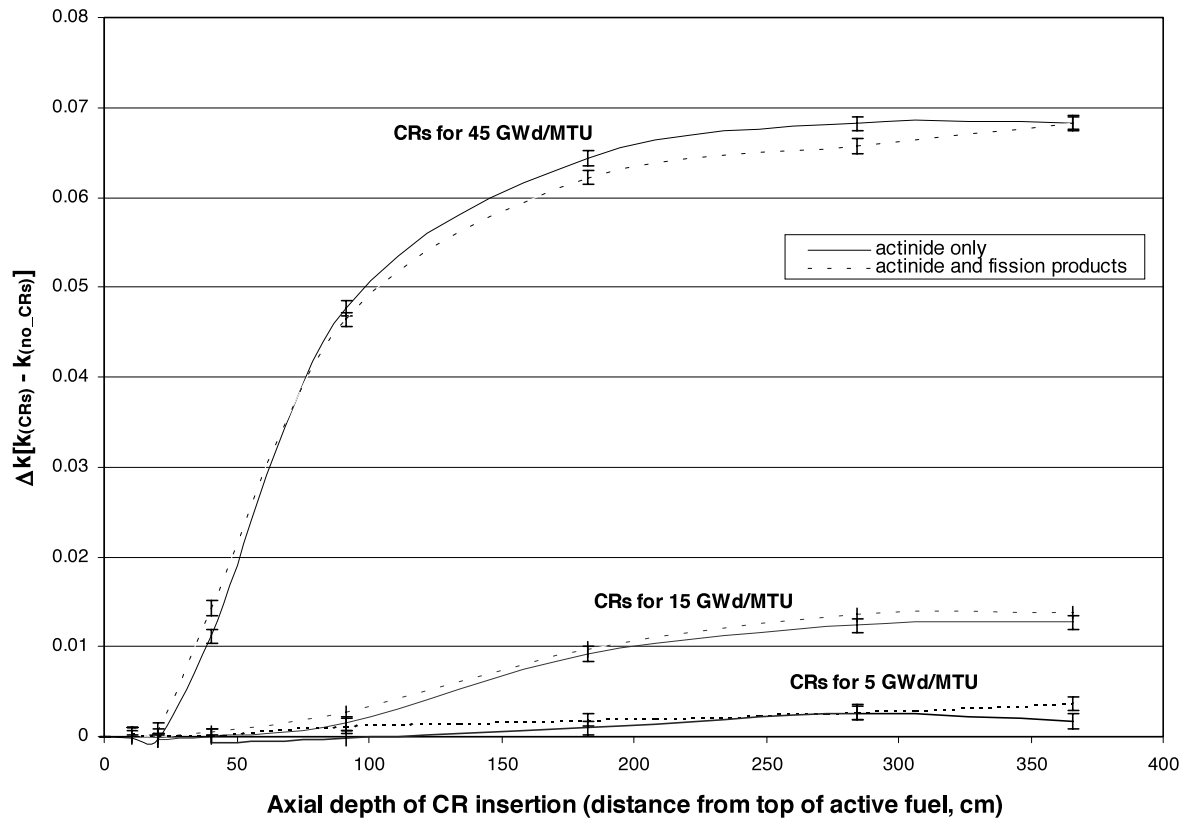


Fig. 32. The  $\Delta k$  values in the GBC-32 cask (45 GWd/tonne U, zero cooling) versus axial CR insertion, as calculated with KENO V.a based on isotopics from HELIOS for actinide-only and actinide + fission product burnup credit. The results correspond to CE  $14 \times 14$  fuel with 4.0 wt%  $^{235}\text{U}$  initial enrichment and Ag-In-Cd/B<sub>4</sub>C CRs. Error bars correspond to  $1\sigma$  uncertainties in the  $\Delta k$  values.

and cross-section libraries have been demonstrated to predict similar results.

#### ACKNOWLEDGMENTS

This work was performed at Oak Ridge National Laboratory (ORNL) under contract with the Office of Nuclear Regulatory Research of the NRC. The authors acknowledge C. J. Withee of the Spent Fuel Project Office and R. Y. Lee of the Office of Nuclear Regulatory Research for their input during the course of this work. In addition, the authors gratefully acknowledge R. J. Cacciapouti (Duke Engineering and Services), H.-R. Hwang (Korea Power Engineering Company), and J. R. Massari (Constellation Nuclear Services) for their invaluable contributions to this work by supplying fuel data and related information. Finally, the authors would like to express their sincere appreciation for the suggestions, review comments, and discussions on all or parts of this work by C. V. Parks, M. D. DeHart, I. C. Gauld, J. C. Gehin, and R. T. Primm of Oak Ridge National Laboratory.

#### REFERENCES

1. "Standard Review Plan for Dry Cask Storage Systems," NUREG-1536, U.S. Nuclear Regulatory Commission (Jan. 1997).
2. "Standard Review Plan for Transportation Packages for Spent Nuclear Fuel—Draft Report for Comment," NUREG-1617, U.S. Nuclear Regulatory Commission (Mar. 1998).
3. "Interim Staff Guidance—8, Rev. 1—Limited Burnup Credit," U.S. Nuclear Regulatory Commission, Spent Fuel Project Office (July 1999).
4. "Standard Review Plan for Transportation Packages for Spent Nuclear Fuel—Final Report," NUREG-1617, U.S. Nuclear Regulatory Commission (Mar. 2000).
5. D. E. CARLSON, C. J. WITHEE, and C. V. PARKS, "Spent Fuel Burnup Credit in Casks: An NRC Perspective," *Proc. 27th Water Reactor Safety Information Mtg.*, Bethesda, Maryland, October 25–27, 1999, NUREG/CP-0169, p. 419, U.S. Nuclear Regulatory Commission (Mar. 2000).

6. C. E. SANDERS and J. C. WAGNER, "Study of the Effect of Integral Burnable Absorbers for PWR Burnup Credit," NUREG/CR-6760, ORNL/TM-2000/321, Oak Ridge National Laboratory (Mar. 2002).
7. J. C. WAGNER and C. V. PARKS, "Parametric Study of the Effect of Burnable Poison Rods for PWR Burnup Credit," NUREG/CR-6761, ORNL/TM-2000/373, Oak Ridge National Laboratory (Mar. 2002).
8. C. E. SANDERS and J. C. WAGNER, "Parametric Study of the Effect of Control Rods for PWR Burnup Credit," NUREG/CR-6759, ORNL/TM-2001/69, Oak Ridge National Laboratory (Feb. 2002).
9. J. J. CASAL, R. J. J. STAMM'LER, E. A. VILLARINO, and A. A. FERRI, "HELIOS: Geometric Capabilities of a New Fuel-Assembly Program," *Proc. Int. Topl. Mtg. Advances in Mathematics, Computations, and Reactor Physics*, Pittsburgh, Pennsylvania, April 28–May 2, 1991, Vol. 2, p. 10.2.1 113.
10. M. D. DeHART, "Sensitivity and Parametric Evaluations of Significant Aspects of Burnup Credit for PWR Spent Fuel Packages," ORNL/TM-12973, Oak Ridge National Laboratory (May 1996).
11. L. M. PETRIE and N. F. LANDERS, "KENO V.a: An Improved Monte Carlo Criticality Program with Supergrouping," *SCALE: A Modular Code System for Performing Standardized Computer Analyses for Licensing Evaluation*, Vol. II, Sec. F11, available from Radiation Safety Information Computational Center at Oak Ridge National Laboratory as CCC-545 (May 2000).
12. *SCALE: A Modular Code System for Performing Standardized Computer Analyses for Licensing Evaluation*, available from Radiation Safety Information Computational Center at Oak Ridge National Laboratory as CCC-545 (May 2000).
13. "Topical Report on Actinide-Only Burnup Credit for PWR Spent Nuclear Fuel Packages," DOE/RW-0472, Rev. 2, U.S. Department of Energy, Office of Civilian Radioactive Waste Management (Sep. 1998).
14. C. V. PARKS, M. D. DeHART, and J. C. WAGNER, "Review and Prioritization of Technical Issues Related to Burnup Credit for LWR Fuel," ORNL/TM-1999/303, Oak Ridge National Laboratory (Feb. 2000).
15. M. A. TREMBLAY and J. P. GORSKI, "Seabrook Station Cycle 5 Nuclear Design Report," YAEC-1927, Yankee Atomic Electric Company (Nov. 1995).
16. R. J. CACCIAPOUTI and S. VAN VOLKINBURG, "Axial Burnup Profile Database for Pressurized Water Reactors," Yankee Atomic Electric Company (May 1997).
17. M. SCHLIECK, H.-D. BORGER, and A. NEUFERT, "Optimized Gadolinia Concepts for Advanced In-Core Fuel Management in PWRs," *Nucl. Eng. Des.*, **205**, 191 (2001).
18. "System Description for Reactor Core for Ulchin 5 & 6 Nuclear Power Plants," N0696-RE-SD280, Korean Power Engineering Company (1997).
19. "Calvert Cliffs Nuclear Power Plant UFSAR," Rev. 26, Constellation Nuclear.
20. J. C. WAGNER, "Computational Benchmark for Estimation of Reactivity Margin from Fission Products and Minor Actinides in PWR Burnup Credit," ORNL/TM-2000/306, Oak Ridge National Laboratory (Oct. 2001).
21. C. V. PARKS, I. C. GAULD, J. C. WAGNER, B. L. BROADHEAD, M. D. DeHART, and D. D. EBERT, "Research Supporting Implementation of Burnup Credit in the Criticality Safety Assessment of Transport and Storage Casks," *Proc. 28th Water Reactor Safety Information Mtg.*, Bethesda, Maryland, October 23–25, 2000, NUREG/CP-0172, p. 139, U.S. Nuclear Regulatory Commission (May 2001).
22. J. C. WAGNER and M. D. DeHART, "Review of Axial Burnup Distribution Considerations for Burnup Credit Calculations," ORNL/TM-1999/246, Oak Ridge National Laboratory (Feb. 2000).
23. P. M. O'LEARY and M. L. PITTS, "Effects of Integral Burnable Absorbers on PWR Spent Nuclear Fuel," *Trans. Am. Nucl. Soc.*, **83**, 128 (2000).
24. B. H. WAKEMAN and S. A. AHMED, "Evaluation of Burnup Credit for Dry Storage Casks," EPRI NP-6494, Electric Power Research Institute (Aug. 1989).
25. "CRWMS M&O 1998 Summary Report of Commercial Reactor Criticality Data for Sequoyah Unit 2," B00000000-01717-5705-00064 Rev. 01, Las Vegas, Nevada: CRWMS M&O. MOL.19980716.0015, U.S. Department of Energy.
26. S. M. BOWMAN, O. W. HERMANN, and M. C. BRADY, "SCALE-4 Analysis of Pressurized Water Reactor Critical Configurations: Vol. 2—Sequoyah Unit 2 Cycle 3," ORNL/TM-12294, Vol. 2, Oak Ridge National Laboratory (Mar. 1995).
27. S. M. BOWMAN and O. W. HERMANN, "SCALE-4 Analysis of Pressurized Water Reactor Critical Configurations: Vol. 3—Surry Unit 1 Cycle 2," ORNL/TM-12294, Vol. 3, Oak Ridge National Laboratory (Mar. 1995).
28. S. M. BOWMAN and T. SUTO, "SCALE-4 Analysis of Pressurized Water Reactor Critical Configurations: Vol. 5—North Anna Unit 1 Cycle 5," ORNL/TM-12294, Vol. 5, Oak Ridge National Laboratory (Oct. 1996).
29. "Summary Report of Commercial Reactor Criticality Data for Crystal River Unit 3," B00000000-01717-5705-00060 Rev. 01, Las Vegas, Nevada: CRWMS M&O. MOL.19980728.0189, U.S. Department of Energy (Apr. 16, 1998).
30. "Characteristics of Spent Fuel, High-Level Waste, and Other Radioactive Wastes Which May Require Long-Term Isolation," DOE/RW-0184, Vol. 1, U.S. Department of Energy (Dec. 1987).
31. "Characteristics of Potential Repository Wastes," DOE/RW-0184-R1, Vol. 1 (July 1992).

32. O. W. HERMANN and C. V. PARKS, "SAS2H: A Coupled One-Dimensional Depletion and Shielding Analysis Module," *SCALE: A Modular Code System for Performing Standardized Computer Analyses for Licensing Evaluation*, Vol. I, Sec. S2, available from Radiation Safety Information Computational Center at Oak Ridge National Laboratory as CCC-545 (May 2001).
33. T. L. SANDERS and R. M. WESTFALL, "Feasibility and Incentives for Burnup Credit in Spent Fuel Transport Casks," *Nucl. Sci. Eng.*, **104**, 66 (1990).
34. "Disposal Criticality Analysis Methodology Technical Report," B00000000-01717-5705-00020, Rev. 00, U.S. Department of Energy (Aug. 1996).
35. O. W. HERMANN, S. M. BOWMAN, M. C. BRADY, and C. V. PARKS, "Validation of the SCALE System for PWR Spent Fuel Isotopic Composition Analyses," ORNL/TM-12667, Oak Ridge National Laboratory (Mar. 1995).
36. M. D. DeHART and O. W. HERMANN, "An Extension of the Validation of SCALE (SAS2H) Isotopic Predictions for PWR Spent Fuel," ORNL/TM-13317, Oak Ridge National Laboratory (Sep. 1996).
37. M. RAHIMI, E. FUENTES, and D. LANCASTER, "Isotopic and Criticality Validation for PWR Actinide-Only Burnup Credit," DOE/RW-0497, U.S. Department of Energy (May 1997).
38. J. C. WAGNER, "Addressing the Axial Burnup Distribution in PWR Burnup Credit Criticality Safety," *Proc. Topl. Mtg. Practical Implementation of Nuclear Criticality Safety*, Reno, Nevada, November 11–15, 2001, American Nuclear Society (2001) (CD-ROM).
39. M. MAILLOT, E. GUILLOU, D. BIRON, and S. JANSKI, "Search for an Envelope Axial Burnup Profile for Use in PWR Criticality Studies with Burnup Credit," *Proc. ICNC'99, 6th Int. Conf. Nuclear Criticality Safety*, Versailles, France, September 20–24, 1999.
40. M. D. DeHART, "SCALE-4 Analysis of Pressurized Water Reactor Critical Configurations: Vol. 4—Three Mile Island Unit 1 Cycle 5," ORNL/TM-12294, Vol. 4, Oak Ridge National Laboratory (1995).

---

**John C. Wagner** (BS, nuclear engineering, University of Missouri-Rolla, 1992; MS, 1994, and PhD, 1997, nuclear engineering, The Pennsylvania State University) is a research and development staff member in the Nuclear Analysis Methods and Applications group of the Nuclear Science and Technology Division (NSTD) at Oak Ridge National Laboratory (ORNL). For the last several years, he has been involved in research and analyses related to criticality safety for spent-fuel storage, transportation, and disposal, with particular focus on burnup credit. His research interests include criticality safety, radiation shielding, reactor physics, and Monte Carlo methods.

**Charlotta E. Sanders** (BS, mechanical engineering, Brigham Young University, 1994; MS, nuclear engineering, Texas A&M University, 1995; ScD, nuclear and reactor physics, Royal Institute of Technology, Sweden, 1999) is a postdoctoral research associate in NSTD at ORNL, where she is involved in research related to burnup credit for spent-fuel storage and transport. Her research interests, in addition to burnup credit, include criticality safety and reactor physics.